REPORT DOCUMENTATION PAGE	READ INSTRUCTIONS BEFORE COMPLETING FORM
1. REPORT NUMBER **AD-A154 894** 2. GOVT ACCESSION NO.	3. RECIPIENT'S CATALOG NUMBER
4. TITLE (and Subtitle) Impact Strength Analysis of a Riveted Joint in the M240 Machine Gun	5. TYPE OF REPORT & PERIOD COVERED Final Report May 1985
	6. PERFORMING ORG. REPORT NUMBER
7. AUTHOR(s) Bowles, Floyd Everett	8. CONTRACT OR GRANT NUMBER(s)
9. PERFORMING ORGANIZATION NAME AND ADDRESS Student,HQDA,MILPERCEN (DAPC-OPA-E), 200 Stovall Street, Alexandria, Virginia 22332	10. PROGRAM ELEMENT, PROJECT, TASK AREA & WORK UNIT NUMBERS
11. CONTROLLING OFFICE NAME AND ADDRESS HQDA, MILPERCEN, ATTN: DAPC-OPA-E, 200 Stovall Street, Alexandria, Virginia 22332	12. REPORT DATE May 1985
	13. NUMBER OF PAGES 99
14. MONITORING AGENCY NAME & ADDRESS(If different from Controlling Office)	15. SECURITY CLASS. (of this report) Unclassified
	15a. DECLASSIFICATION/DOWNGRADING SCHEDULE

16. DISTRIBUTION STATEMENT (of this Report)

Approved for public release; distribution unlimited.

17. DISTRIBUTION STATEMENT (of the abstract entered in Block 20, if different from Report)

"Original contains color plates: All DTIC reproductions will be in black and white"

18. SUPPLEMENTARY NOTES

This document is a thesis in partial fulfillment of the degree of Master of Science in Mechanical Engineering from Purdue University, West Lafayette, IN 47906.

19. KEY WORDS (Continue on reverse side if necessary and identify by block number)

Small arms weapon design, strength analysis, fatigue analysis, impact, stress, finite element analysis.

20. ABSTRACT (Continue on reverse side if necessary and identify by block number)

A proposed modification of the shape of a slot in the inner wall of the lower receiver of the M240 machine gun is investigated to determine the effect of the change on the life of the weapon. The slot helps provide restraint for the locking shoulders which support the rearward thrust of the bolt and bolt carrier. Impact and fatigue loading are considered. Estimates of the stress in the rivets and restraints of the locking shoulder are made based on (1) the assumption of even distribution of load across areas in

DD FORM 1473   1 JAN 72   EDITION OF 1 NOV 65 IS OBSOLETE

shear, and (2) finite element analysis of the locking shoulder/ rivet/receiver combination. Results of both analyses indicate that the slot can be modified without reducing the life of the weapon.

IMPACT STRENGTH ANALYSIS OF A RIVETED JOINT IN THE M240 MACHINE GUN

CPT Floyd E. Bowles
HQDA, MILPERCEN (DAPC-OPA-E)
200 Stovall Street
Alexandria, VA 22332

Final Report May 1985

A thesis submitted to the faculty of Purdue University, West Lafayette, IN, in partial fulfillment of the requirements for the degree of Master of Science in Mechanical Engineering.

IMPACT STRENGTH ANALYSIS OF A RIVETED JOINT

IN THE M240 MACHINE GUN

A Thesis

Submitted to the Faculty

of

Purdue University

by

Floyd Everett Bowles

In Partial Fulfillment of the

Requirements for the Degree

of

Master of Science in Mechanical Engineering

May 1985

This research, like all I am given charge of,

is dedicated to our Lord Jesus Christ,

in faith that He has assured its proper application.

ACKNOWLEDGEMENTS

TABLE OF CONTENTS

LIST OF TABLES

LIST OF FIGURES

The bolt mass M_1 is driven by a drive spring K_1 and encounters a cartridge located initially at rest at position X_a. These two masses are subsequently locked together during continued motion and seating of the round. At position X_b the pair of masses encounters resistance at the bolt face, represented by a stiff spring K_2. Modeling of this motion requires the following system of pieced differential equations, which are valid only in separate intervals of position:

$$M_1 \ddot{X} + K_1(X - l_o) = 0 \qquad (2.4)$$
$$X < X_a$$
$$(M_1 + M_2)\ddot{X} + K_1(X - l_o) = 0 \qquad (2.5)$$
$$X_a < X < X_b$$
$$(M_1 + M_2)\ddot{X} + K_1(X - l_o) + K_2(X - X_o) = 0 \qquad (2.6)$$
$$X > X_b$$

The complexity of a complete model of a weapon, therefore, normally requires isolation of the part of the weapon to be studied and certain simplifying assumptions must be made to arrive at a useful solution. This is the approach taken in determining the force applied to the locking shoulder in this research.

2.3 Description of the M240 Machine Gun

An exploded view of the M240 machine gun is shown in Figure 2.2 [5]. The receiver (1) is mounted to the tank by

model with the applied load being the gas pressure inside the barrel and the chamber. Although this method gives accurate results it is expensive in terms of computation time and resources.

The discontinuous nature of some of the forces and masses further complicates the problem of constructing a model of the entire weapon undergoing a cycle of operation. Consider the schematic of the bolt, cartridge, and chamber interface as shown in figure 2.1 [4], which is used to demonstrate these discontinuities in the operation of load-ing the weapon.
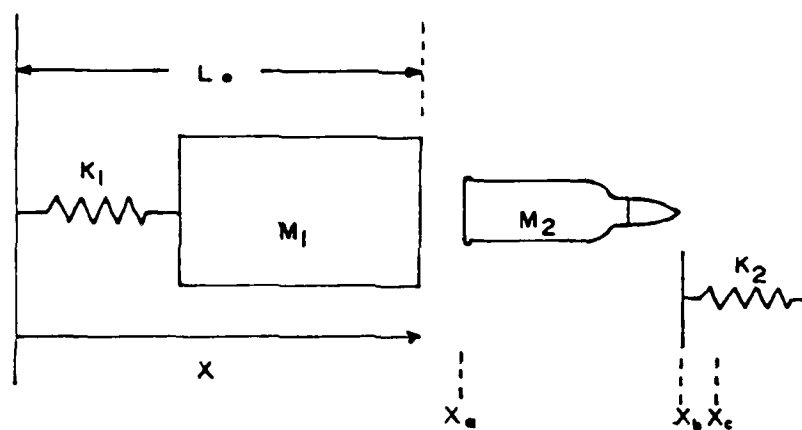
Figure 2.1 Bolt, Cartridge, and Chamber Schematic

$$M_{op}\ddot{X} = F_{drive\ spring} - F_{gravity\ on\ op} - \quad (2.2)$$

$$F_{dynamic\ friction} - F_{feed\ pawl} - F_{delink} - F_{lock} -$$

$$F_{impact} - F_{constraint} - F_{gas} + F_{unlock} +$$

$$F_{belt\ feed} - F_{blowback} + F_{cartridge\ case\ drag} +$$

$$F_{eject} + F_{rear\ plate\ impact}$$

Each of the force terms (denoted by F with subscript) must be approximated theoretically or derived from experimental measurement. The nonlinearity of the equations is indicated in one of these terms, the force F_{mount} applied to the main gun by the mount:

$$F_{mount} = C_1 + C_2 X_{mg} + C_3 \dot{X}_{mg} + \quad (2.3)$$

$$C_4 \ddot{X}_{mg} + C_5 \dot{X}_{mg} X_{mg} +$$

$$C_6 \dot{X}_{mg} \ddot{X}_{mg} + C_7 X_{mg} \ddot{X}_{mg} +$$

$$C_8 X_{mg} \dot{X}_{mg} \ddot{X}_{mg} + C_9 X_{mg}^3$$

where C_1 through C_9 are constants that depend upon the mount used. Some of the other force terms are nonlinear also.

A different approach was taken by M.T. Soifer [3] for a model of the 75 mm ADMAG gun system. In this case the entire weapon with its moving parts was considered to be a collection of 19 finite elements, each with 6 degrees of freedom, giving the entire weapon 114 degrees of freedom. To determine a force at a particular location inside the weapon mechanism required the solution of a finite element

2.2 Mathematical Models of Automatic Weapon Systems

Past research on the transmission of forces from one part of a weapon to another shows that the problem can quickly become very complex, employing models with many degrees of freedom, even when simplifying assumptions have been made.

Ehle [2] gives an example of the complexity of the mathematical model of a gas operated automatic weapon. He has simplified these models and assumed two degrees of freedom - translation of the operating parts, designated OP in the equations, and translation of the main gun, designated MG. This was done because other motions in the gun have relatively small effect and may be neglected without significantly affecting results.

Ehle proposes the following equations of motion corresponding to the two degrees of freedom.

$$M_{mg}\ddot{X} = F_{mount} - F_{drive\ spring} - F_{gravity} + \quad (2.1)$$
$$F_{friction} + F_{feed\ pawl} + F_{delink} + F_{lock} +$$
$$F_{barrel\ impact} + F_{constraint} + F_{gas\ on\ mg} +$$
$$F_{bore\ friction} - F_{breech\ pressure} - F_{unlock} -$$
$$F_{belt\ feed} - F_{cartridge\ case\ drag} - F_{eject} -$$
$$F_{rear\ plate\ impact}$$

the bore a few milliseconds after the projectile has cleared the muzzle. Friction between the cartridge and chamber wall combined with the inertia of a relatively large bolt help hold the cartridge in place until the projectile leaves the barrel. At that time chamber pressure is reduced enough to allow the cartridge to freely move, and residual pressure is high enough to push the bolt/cartridge combination to the rear. Problems arise in the control of the rearward velocity of the bolt. Generally, pure blow-back operation requires an extremely large bolt mass and is not suitable for use in a high powered automatic weapon.

Gas operation is a method by which some of the propellant gasses are routed through a hole halfway down the barrel into a gas cylinder. Pressure on a piston inside the gas cylinder forces the piston to the rear, which in turn pushes an operating rod to the rear, actuating the mechanism which ejects the spent cartridge. A spring is compressed by the operating rod as it travels to the rear. This spring pushes the operating rod forward once the old cartridge is extracted which in turn carries the bolt forward to rechamber a new round of ammunition from the ammunition belt.[1] This method of operation has proven to be the most suitable for use in small arms and is the method used in the M240 machine gun.

CHAPTER 2 - DETERMINATION OF INPUT FORCE

2.1 Introduction - Automatic Weapon Mechanism Types

In all fully automatic weapons the source of force applied to the internal parts and the mount is the propellant gas behind the projectile upon firing a round of ammunition. This source of power may be tapped in one of two ways; (1) by using the rearward thrust of the recoiling mass; and (2) by using the pressure generated in the bore by the expanding gas of the progressive burning charge. The former is known as recoil actuation, while the latter is labeled gas operation.[1]

Recoil actuation is limited in its utility. The only significant application in use today with small caliber weapons is the M2 .50 caliber Browning heavy barrel machine gun. Generally, recoil actuation is slow and requires a large caliber projectile to produce enough recoil to operate the weapon. [1]

Gas operation, however, seems to be almost unlimited in its application. Two major categories of gas operation exist. They are referred to as blowback and gas operation. Blowback makes use of the residual pressure remaining in

methods to estimate the type of error introduced by this assumption.

4. Recommendations for design change are made based on findings outlined above, and the results of the two models are compared.

1.3 Description of Research

Included in this thesis are the following:

1. A simple model of the mechanism is developed to determine the forcing function applied to the face of the locking shoulder by the bolt. This includes a description of the mechanism and one cycle of operation based on interior ballistics data.

2. An estimate of the strength of the fasteners and restraints for the original and modified slot geometry is made using traditional analysis methods for riveted joints. Material strength estimates account for fatigue and impact stress factors.

3. A finite element model of the locking shoulder and rivets is used to determine locations of high stress concentration of the locking shoulder/rivet combination. The value of stress at these locations will be compared with that predicted by the preliminary model in 2. above.

Finite element modeling is used because the common assumption made in the analysis of riveted joints is that each restraint carries the same load per unit area in shear. This assumption is valid if both parts are very stiff relative to the rivets and the restraints. This may not be the case here. Therefore, an additional objective of this research is to compare the results of the two
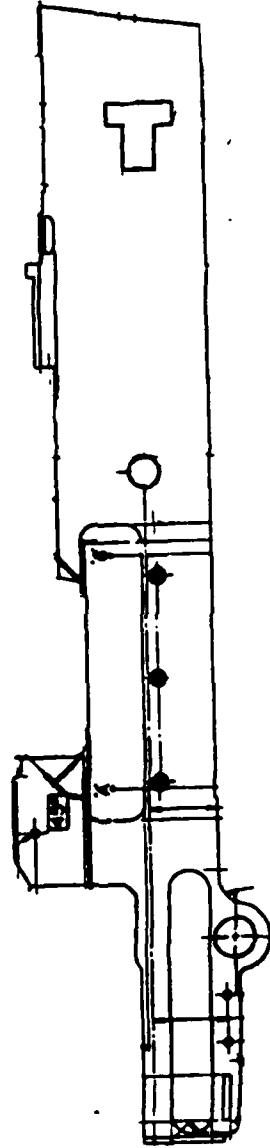
Figure 1.2 Inside of Receiver Wall

4
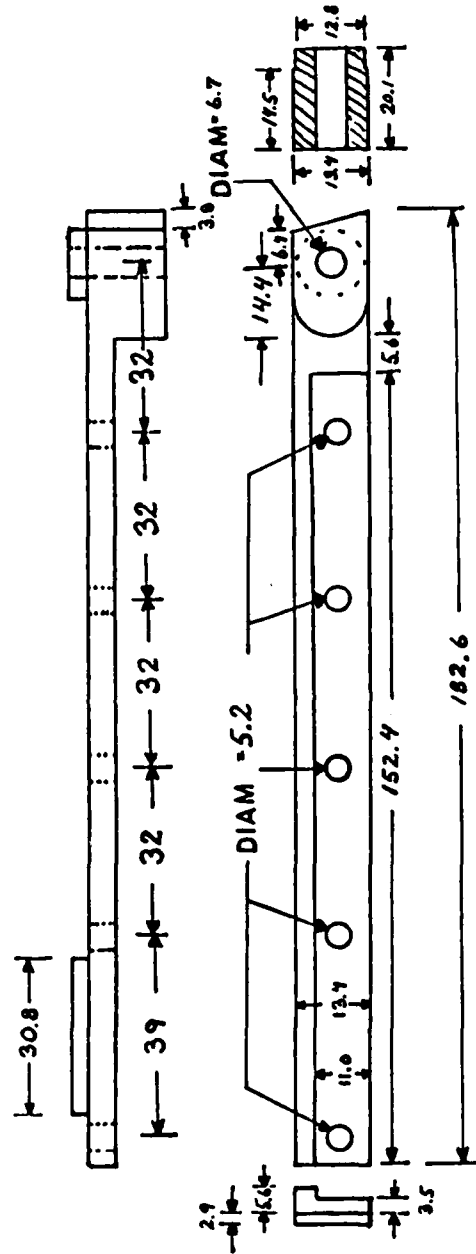
Figure 1.1 Locking Shoulder Dimensions and Geometry

such that the restraints at the front and rear have enough shear area to hold the applied force. The purpose of the rivets is to hold the shoulder firmly in place.

The T-shaped slot shown in figure 1.2 is carved into the receiver wall where the rear restraint of the locking shoulder is held. It is the T-slot area that is causing difficulty in the assembly process, and the desire is to change the shape of the slot to a rectangle, thus providing horizontal restraint but eliminating any vertical restraint contributed by the slot.

Of concern is whether the lack of vertical restraint in the T-slot area will allow excessive stress on the last two rivets due to vertical displacement of the locking shoulder. The performance of the weapon has exceeded original design specifications and before any changes are made there should be strong evidence that the proposed changes do not detract from that performance. This research, there-fore, is a more detailed study of the proposed change.

series tank. In the M240 machine gun the structural com-
ponent in the receiver that holds the bolt against the base
of the cartridge in the chamber is called the locking
shoulder.

1.2 Problem Statement

The United States Army Armament, Munitions, and Chemi-
cal Command (AMCCOM) at Rock Island, Illinois is currently
considering a modification to the structure of the locking
shoulder and receiver in the M240 machine gun. The locking
shoulder is mounted inside the lower receiver by six
rivets. Force is applied to the locking shoulder face which
causes stress to be felt by the rivets and two restraints
that are a part of the locking shoulder.

To make assembly easier, AMCCOM would like to change
the shape of a slot in the receiver wall that holds one of
the restraints. If the shape of the slot can be altered
without causing excessive stress in either of the res-
traints or any of the six rivets, the manufacturing process
can be made easier and less expensive.

Consider figures 1.1 and 1.2. The locking shoulder is
held in place against the inside wall of the lower receiver
of the weapon by six rivets. Force is applied to the face
of the shoulder by the bolt and bolt carrier when a round
of ammunition is fired. The locking shoulder is designed

CHAPTER 1 - INTRODUCTION

1.1 Background

The mechanism and structure of a small caliber weapon system consists of several parts that either move or resist the motion that results from the force input from an exploding charge. In a fully automatic system the mechanism is designed to hold the cartridge in the chamber while pressure from the powder gasses is greater than zero. Once the pressure in the chamber subsides, the spent cartridge is extracted and discarded, and a new round of ammunition is fed into the chamber.

The item that holds the cartridge in the chamber is called the bolt. The bolt is restrained against the structure of the receiver for the period of time required to hold the cartridge in place. The mechanism is designed to release the bolt from the restraint when it becomes necessary to extract the cartridge.

The M240 machine gun is a 7.62 mm (approximately .30 caliber) tank mounted anti-personnel weapon used by many NATO countries. It was designed in Belgium and adopted in the late 1970's for use by American forces on the M60

ABSTRACT

Bowles, Floyd Everett. MSME, Purdue University. May 1985. Impact Strength Analysis of a Riveted Joint in the M240 Machine Gun. Major Professor: Dr. J.M. Starkey, School of Mechanical Engineering

A proposed modification of the shape of a slot in the inner wall of the lower receiver of the M240 machine gun is investigated to determine the effect of the change on the life of the weapon. The slot helps provide restraint for the locking shoulders which support the rearward thrust of the bolt and bolt carrier. Impact and fatigue loading are considered. Estimates of the stress in the rivets and restraints of the locking shoulder are made based on (1) the assumption of even distribution of load across areas in shear, and (2) finite element analysis of the locking shoulder/rivet/receiver combination. Results of both analyses indicate that the slot can be modified without reducing the life of the weapon.

large pins at locations (a) and (b). In this research the receiver/tank combination is considered to be the reference frame for the motion of the operating parts.

The locking shoulders are mounted inside the receiver (1). Figures 2.3 and 2.4 show how they are positioned.

The locking shoulder is made of AISI 9310H modified steel. The rivets that hold the locking shoulder in place consist of the softer AISI 1010 or 1018 carbon steel [6].

Receiver assembly (1)
Feed tray (2)
Cover assembly (3)
Tray and cover axis
pin (4)
Trigger and frame
assembly (5)
Spring trigger pin (6)
Bolt and operating
rod assembly (7)
Driving spring
assembly (8)
Buffer assembly (9)
Barrel assembly (10)
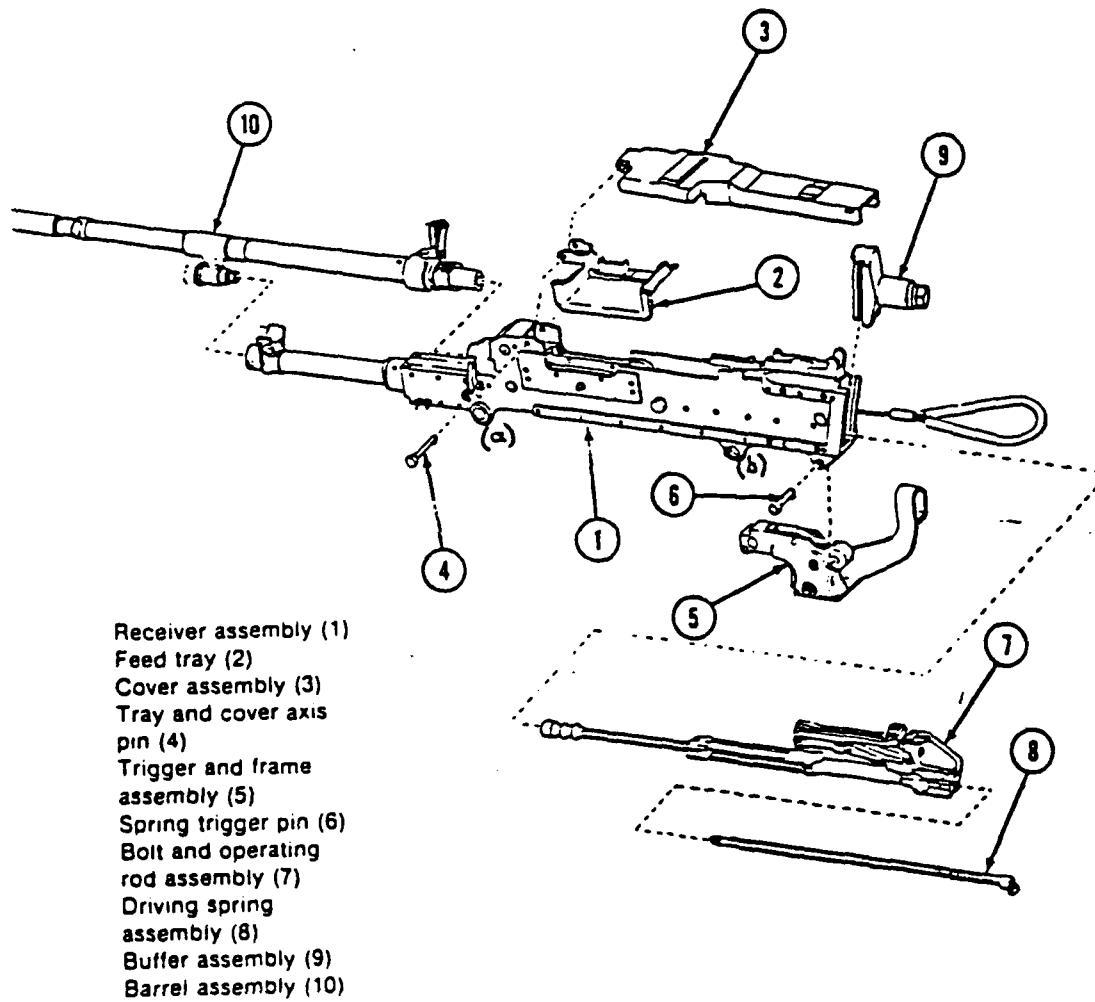
Figure 2.2   Exploded View of M240 MG [5]
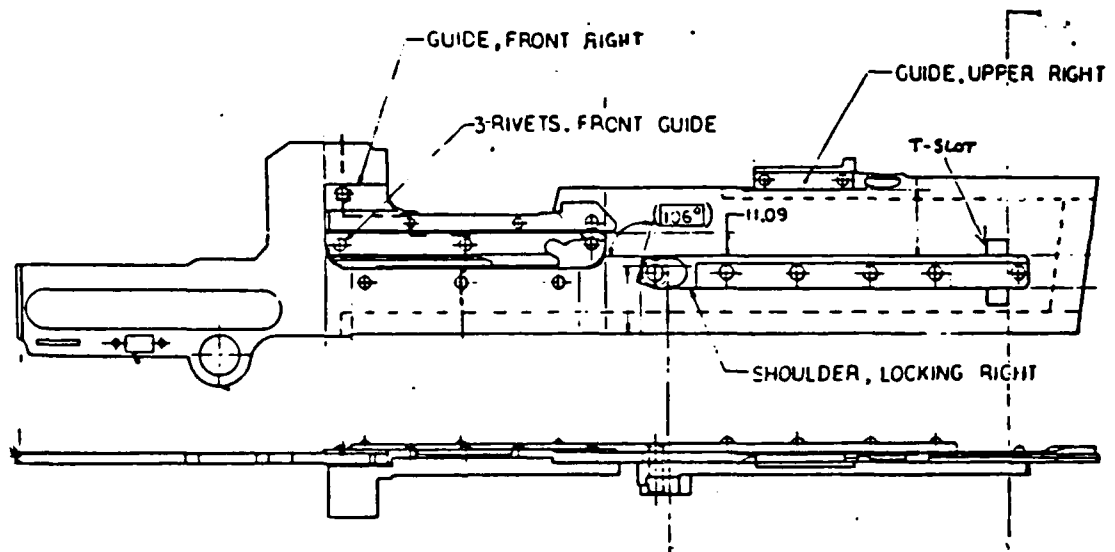
Figure 2.3   Locking Shoulder Position
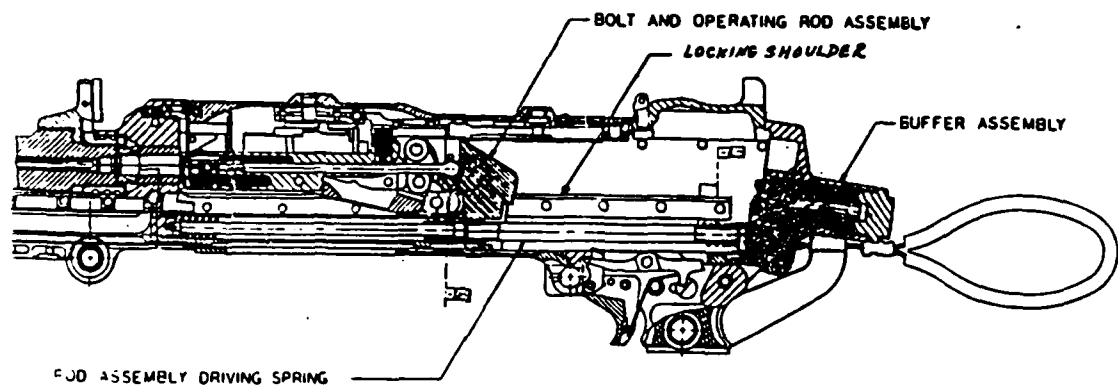
Figure 2.4 Gun Mechanism

2.4 Description of Mechanism Action

The following description of a cycle of operation refers to figures 2.5 through 2.8. The positions of the bolt and bolt carrier shown in figure 2.7 correspond to the position of the operating rod described by figure 2.8.

Before a cycle of operation begins a round is chambered, the bolt is forced against the base of the round, and the bolt assembly is braced rearward against the face of the locking shoulders. Upon pulling the trigger, a spring mechanism is released that causes the firing pin to ride forward with enough force to cause the round to discharge. The cycle begins (t=0) upon discharge of the round.

At approximately t=.2 msec pressure from the discharge of the round is high enough to produce a force on the bullet large enough to overcome friction and the bullet begins to travel through the barrel (figure 2.5). Chamber pressure reaches maximum (P_{max}) extremely quickly such that $P = P_{max} = 52,000$ psi at t = .65 msec [6].

The bolt remains braced against the chamber. The arms of the bolt assembly hold the bolt there being braced against the locking shoulders at a 16 degree angle from the horizontal (Figure 2.7a).
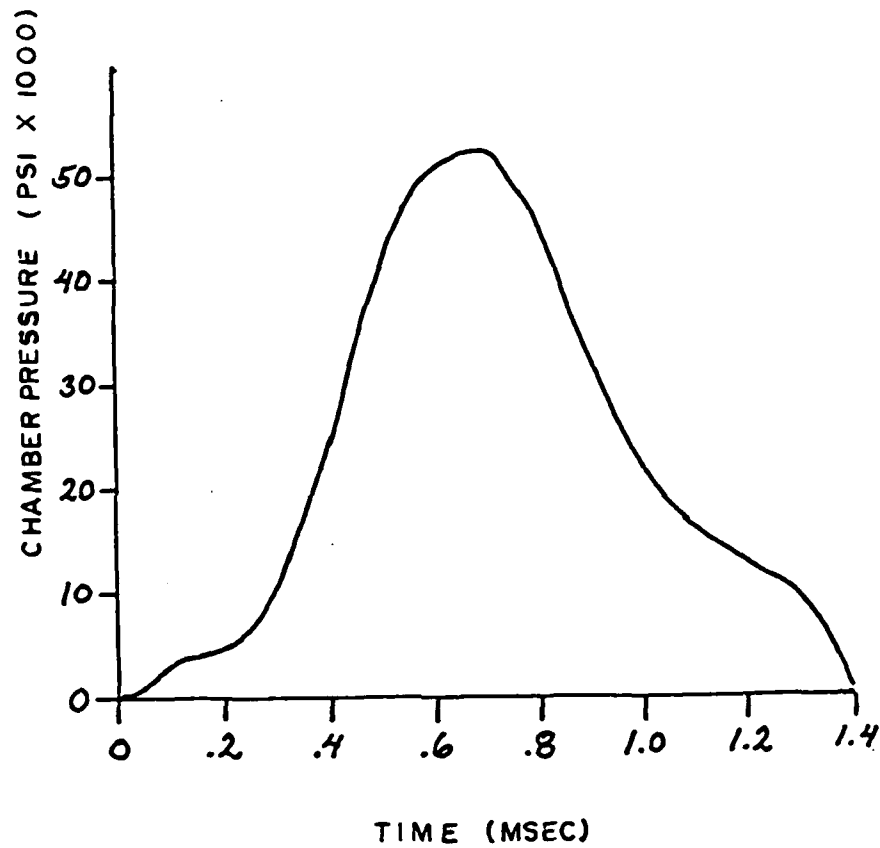
Figure 2.5   Interior Ballistics Data - Pressure vs. Time
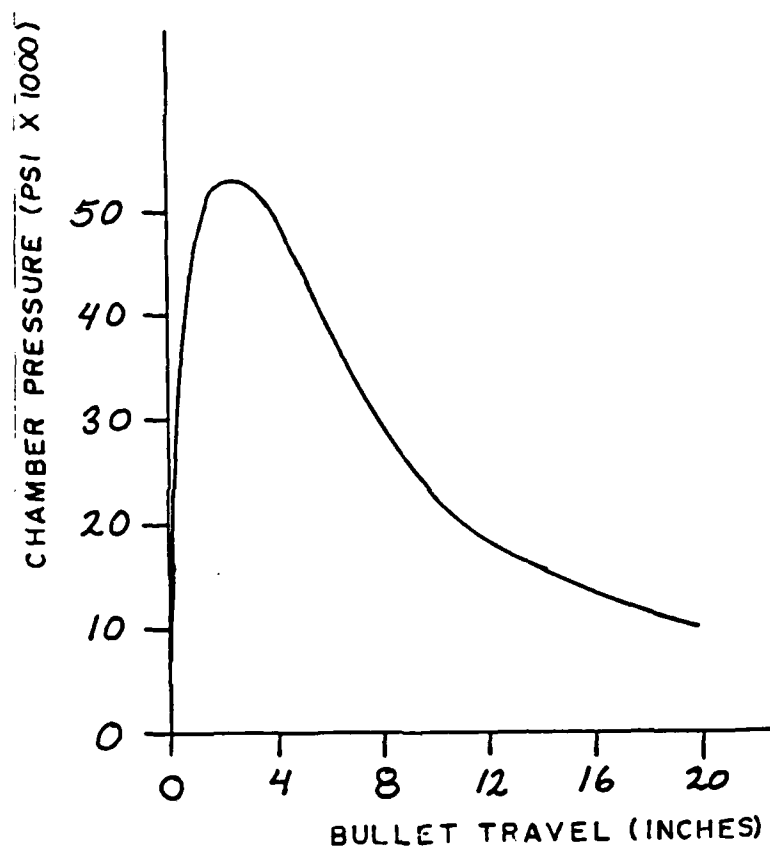
Figure 2.6 Interior Ballistics Data - Pressure vs. Distance

(a)

CHAMBER
OPERATING
ROD

BOLT
ASSEMBLY

LOCKED POSITION

(b)

C

B

A

UNLOCKED POSITION

(c)

FULLY EXTENDED POSITION
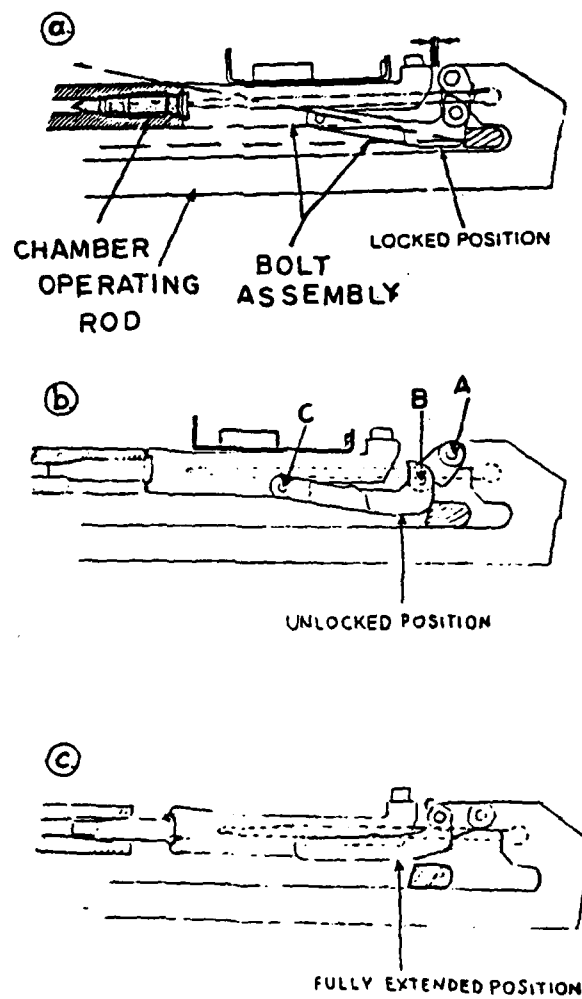
Figure 2.7 Bolt Assembly Motion
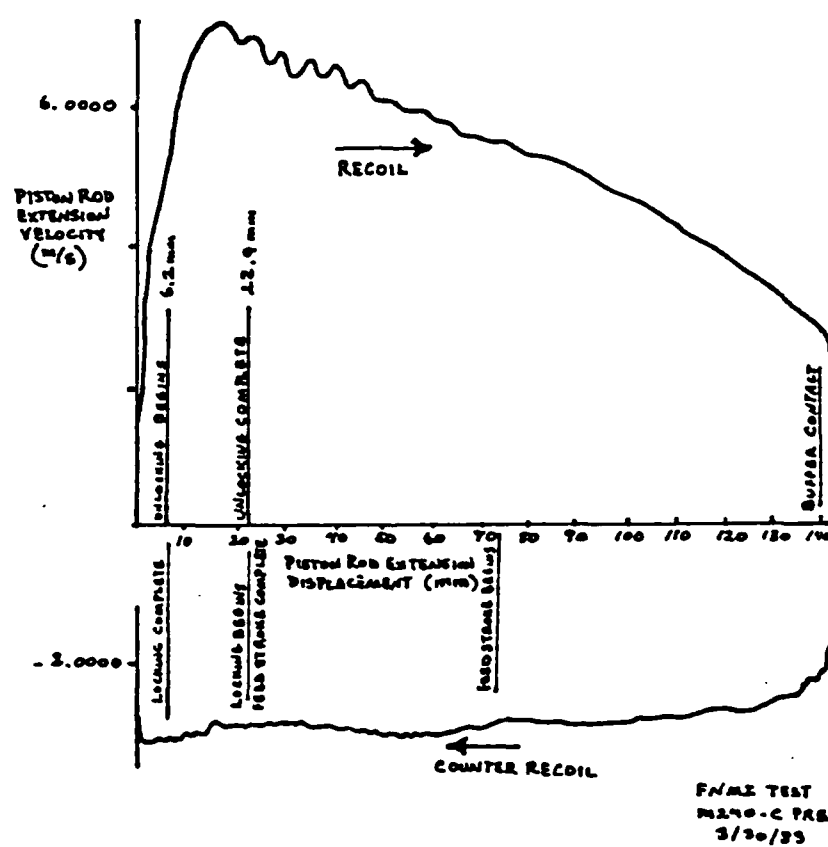
Figure 2.8 Operating Rod Velocity vs. Displacement [6]

At the same time as the pressure of the powder gasses drives the projectile and gasses through the bore, the entire gun mechanism is driven to the rear in recoil. Recoil acceleration is limited by the mass of the recoiling parts, in this case, the mass of the entire weapon and its mount. Since the mount is extremely stiff (large diameter pins mount the weapon to an M1 or M60 tank) the weapon/mount combination is considered in this case to be one item.

As the projectile passes the gas port, powder gasses begin to flow into the gas cylinder and start to drive the operating rod to the rear. The cycle described by figure 2.8 begins at this time. Pressure in the chamber continues to push the projectile toward the muzzle as pressure in the gas port simultaneously pushes the operating rod rearward.

When the operating rod has moved 6.2 mm to the rear it begins to pull the bolt assembly at point A causing link AB to rotate at point A and link BC to rotate at point C (Figure 2.7b and Figure 2.8). Link BC (the bolt carrier) continues to hold the bolt against the chamber until the operating rod has moved 22.9 mm to the rear, at which time link BC slips off the locking shoulder relieving the restraining force.

The mechanism is designed to insure that the projectile has completely cleared the barrel and residual

pressure in the barrel is almost zero before the bolt carrier is allowed to slip off the locking shoulders. High chamber pressures would rupture the thin walls of the brass cartridge if it were extracted too early. The purpose for the linkage of the bolt, bolt carrier, and operating rod is that they provide a time delay allowing the rearward inertia of the operating rod to extract the round when it is safe to do so.

Figure 2.6 shows that pressure is still approximately 10,000 psi when the bullet reaches the end of the 20 inch barrel. Residual pressure trails off to become nearly zero about .1 msec after the bullet leaves the barrel [1]. Figure 2.5 shows the projectile leaving the barrel at approximately 1.3 msec. Thus the position shown in figure 2.7b occurs at approximately 1.4 msec.

Once the bolt carrier breaks contact with the face of the locking shoulders the force input to the locking shoulders is zero. Figure 2.8 shows that much activity still occurs inside the receiver between positions 2.7b and 2.7c. Of interest in this study, however, is the force felt by the locking shoulder, and the rest of the activity will be ignored.

The amplitude and shape of the forcing function curve is directly proportional to the amplitude and shape of the pressure vs. time curve of Figure 2.5. The length of time

between peaks is determined by the rate of fire of the weapon.

The dynamic interaction of the parts in this mechanism clearly leads to nonlinear models due to the intermittent nature of the contacting parts. The locking shoulder, being the object of the study here, is heavily loaded during the early stages of the firing cycle. The next section describes the method for determining the forcing function input to the locking shoulders.

2.5 Determination of Input Force

2.5.1 Period

As stated earlier, the force applied to the locking shoulder face is a result of the chamber pressure from the explosion of the gunpowder in the cartridge. The cyclic rate of fire is between 650 and 950 rounds per minute [5] giving a minimum forcing frequency, f_{min} = 10.83 Hz, and a maximum frequency, f_{max} = 15.83 Hz.

The variation in rate of fire is due to factors such as amount and type of lubrication on the moving parts of the weapon and differences in amount and type of gunpowder in different rounds of ammunition. The most extreme condition is when $f=f_{max}$. Therefore $f = f_{max}$ = 15.83 Hz will be used as the frequency of the forcing function, giving a period of τ = 63.2 msec

The time, T, that force is applied to the face of the locking shoulder is the same amount of time chamber pressure is greater than zero. From the discussion in the previous section, chamber pressure is greater than zero for about 1.4 msec. Thus $T \simeq 1.4$ msec.

Since a round is fired almost every 63.2 msec, and since for each round the chamber pressure dies away in about 1.4 msec, the forcing function will be approximated as a series of impulses of magnitude equal to f_{max} with a period equal to τ.

2.5.2 Amplitude

The maximum amplitude, f_{max}, of the force on the locking shoulder is determined by the maximum value of chamber pressure, P_{max}, the effective area upon which P_{max} is applied inside the cartridge case, and the static configuration of the contacting parts which transmit the force from the cartridge to the locking shoulder. The contacting parts include the cartridge case, bolt assembly, and locking shoulder face.

P_{max} produced by a standard NATO 7.62 mm round of ammunition is 52,000 psi [5]. To determine the effective area upon which P_{max} is applied consider the cartridge in the chamber shown in Figure 2.9. The small arrows indicate the direction of the force caused by P_{max}.

Forces caused by pressure in the cartridge are depicted in figure 2.10. Due to symmetry all forces in the y and z directions will cancel. Assuming negligible deformation of the cartridge, the resolution of forces in the x direction at the cartridge shoulder is a simple statics problem. The only forces in the x direction that do not cancel are those produced by the pressure acting on the base of the projectile, shown as f_p in figure 2.10, and friction forces.

Friction forces have been neglected for the following reasons.

1. The weapon is assumed to be properly lubricated with oil similar in viscosity to grade SAE 30 motor oil, producing an extremely low coefficient of friction between the cartridge and chamber wall.

2. The presence of any friction will only serve to reduce the applied force on the bolt and neglecting it adds a hidden safety factor to the analysis.

The magnitude of $f_{c_{max}}$ is therefore simply $f_{c_{max}} = P_{max}$ (Cross sectional area of projectile). Since the projectile diameter is 7.:2 mm or .3 inches, the force becomes $f_{c_{max}} \simeq 3676$ lbs.

3.2.4 Determination of Maximum Allowable Stress

Fluctuating load as it exists on the locking shoulder and rivets does not present conditions that are as severe as that found with completely reversing load, since the load is applied in only one direction. Much of the data available from empirical analysis is based on completely reversing load conditions since data is easy to gather using completely reversing fatigue testing machines. To determine the maximum allowable stress in the locking shoulder or rivets, S-N curves based on data obtained in testing using completely reversing load can be used realizing that, again, the results will be conservative.

The generalized S-N curve for wrought steel is shown in figure 3.2, and is used to estimate the maximum allowable stress. The maximum allowable stress is defined as the highest stress that can be reached repeatedly for 10^7 cycles or more without causing failure. From the S-N curve the ratio $\frac{S}{S_u}$ at approximately 10^7 cycles is about .5, where S_u is the ultimate tensile strength of the material, and S is the strength of the material under the given load.

The stress impact factor may be applied at this time to reduce the maximum allowable stress of the material. Future stress calculations will use the maximum load in a static analysis since the impact factor will have already been included in the calculations for maximum part life.

method for practical applications generated the development of the following empirical formula that has proven to give results that are sufficiently accurate [10].

$$K_{i_{exact}} = \sqrt{\frac{W}{W_b} + \frac{2}{3}} + 1 \qquad (3.4)$$

where W_b is the weight of object being impacted, and W is the weight of object impacting.

In the M240 machine gun, the object being impacted is the locking shoulder and the impacting object is the bolt/bolt carrier group. The weight of the bolt/bolt carrier is 175 grams [6]. The weight of the locking shoulder is approximately 114.5 grams, given the average weight density $\gamma = 0.283$ lbm/cubic inch, the dimensions of the locking shoulder from figure 1.1 chapter 1, and appropriate conversion factors. Using these values the impact stress factor is found to be 2.48 .

In comparing the two stress impact factors it is not surprising that the method which takes into account the mass and non-uniformity of stresses in the object gives the higher value. To be conservative in this analysis, the higher value of K_i will be used to adjust the stress values obtained in the force analysis.

or it may be applied to the resulting stress in the structure if the maximum static force is used in the force analysis.

For a suddenly applied load, such as an explosion, where h = 0,

$$K_i = 1 + \sqrt{1 + \frac{0}{\delta_{st}}} \qquad (3.2)$$

$$K_i = 2 \qquad (3.3)$$

Using this method, stress calculated in the static analysis of the part is $\frac{1}{2}$ of the actual stress in the part under impact loading.

3.2.3.2 Empirical Impact Factor

A more exact method of predicting impact stresses takes into account the mass of the struck body and the variation of stress throughout the body as a function of time. Timoshenko [11] presents this more exact method which is summarized by Juvinall [8].

The variation of stress in the body as a function of time is a function of the material properties that govern the velocity of shock waves through the body, and the analysis is similar to the study of vibration through a continuous system. The specific solution to any given problem quickly becomes very complex due to complicated geometry and boundary conditions. The need for a simpler

identical to that produced by the static application of the load multiplied by the impact factor. When the mass of the structure is considered the dynamic deflection curve will contain points of higher local strain than the static deflection curve does. Thus, the peak stresses computed by this method may be seriously low.

Assumption 3 implies that no energy is lost due to friction. Under this assumption the principle of conservation of energy requires that once the impacting body has stopped, its kinetic energy is completely transformed into elastic strain energy of the structure. At this moment the maximum deflection and stress occur. In actual practice the damping that is present may cause results to differ substantially from predictions based on the assumption of negligible damping.

From [8], for the impact caused by one body falling on another,

$$F_e = W\left(1 + \sqrt{1 + \frac{2h}{\delta_{st}}}\right) \qquad (3.1)$$

where F_e is the equivalent force caused by the impact, W is the weight of the falling object, h is the height of fall, and $\delta_{st} = \frac{W}{K}$ is the static deflection of the structure. The term inside the parenthesis is called the impact factor, K_i, and may be applied either to the weight of the falling object, as has been done above to get an equivalent force,

3.2.3 Effect of Impact Loading

The force felt by the locking shoulder face can be modeled as a series of impact loads of magnitude equal to $F_{applied}$. This is a common assumption in weapon design, just as it is in the design of the mechanisms used in internal combustion engines.

Two methods for determining a stress impact factor are presented here. The first is presented for reference since it is simple and commonly used. It is an approximation based on non-conservative assumptions that are often made in the analysis of this type of problem. The second is a more accurate method based on empirical data and is the method used to evaluate the M240 machine gun.

3.2.3.1 Approximate Impact Factor

Juvinall [8] presents a detailed discussion of impact loading. In this analysis the following assumptions are made.

1. The *mass of* the structure being impacted is zero.

2. The deflections within the mass itself are zero.

3. Damping within the structure is zero.

The first assumption implies that the instantaneous dynamic deflection vs. time curve of the structure is

for impact and fatigue to be the failure point stress.

In practice, tensile stresses in the locking shoulder may be extremely small. Rivets are normally driven into place so that they fill the rivet hole and are preloaded in compression. This compressive preloading of the rivet often offsets any tension that would be felt around the rivet hole. Sometimes, however, since rivets are hot when driven and contract upon cooling, the preloading may be reduced or eliminated. The common assumption for analysis purposes is that preloading does not exist, even though it often does, because it is extremely difficult to determine its magnitude. Experience demonstrates that this assumption is acceptable [7 and 10].

As mentioned above, rivets contract upon cooling after insertion into the rivet hole. The shrinkage of the rivet causes the rivet heads to pull the plates together with considerable normal force. The friction due to this force is often very large and under certain conditions carries the entire applied load. Despite the assistance given by friction it is customary to compute the strength of a riveted joint from the strength of the rivets in shear or the tension of the plates between or around the rivet holes [9]. Again, assumptions of this type are acceptable since the presence of friction relieves the rivets and restraints of some of the load they must carry.

is not of major concern. It is the total number of load applications that is the significant factor. Thus the life of a part is described as the number of applications of a certain level load that the part is able to sustain before it fails. Experience indicates that, for ferrous metals, if a part does not fail after 10^7 applications of a given load, it can be assumed that the part has infinite life at that particular load [8].

Although it is possible to have fatigue failure in a region of compressive stress, failures usually occur under tensile stress at levels considerably lower than those in a compressive stress failure [7]. Therefore, the maximum allowable tensile stress for the type of steels used will be adjusted for fatigue and impact conditions and the result used to determine the life of the part.

3.2.2 Rivets Under Transverse Loading

Rivets under transverse loading experience a combination of normal and shear stresses. In the design of weapon components the von Mises-Hencky maximum distortion energy theory of failure has proven to be very accurate when compared to experimental results [9]. The Mohr's circle equations will be used to determine the principle stresses from the normal and shear stresses. The principle stresses are then used in the von Mises-Hencky theory to predict failure by assuming maximum tensile stress of the material adjusted

The type of loading felt by the face of the locking shoulder, however, is not completely reversing, but is called fluctuating load. This type of loading is characterized by a changing magnitude without necessarily changing the direction of load application. Figure 3.1 illustrates this difference.

TIME
FLUCTUATING LOAD

TIME
COMPLETELY REVERSING LOAD
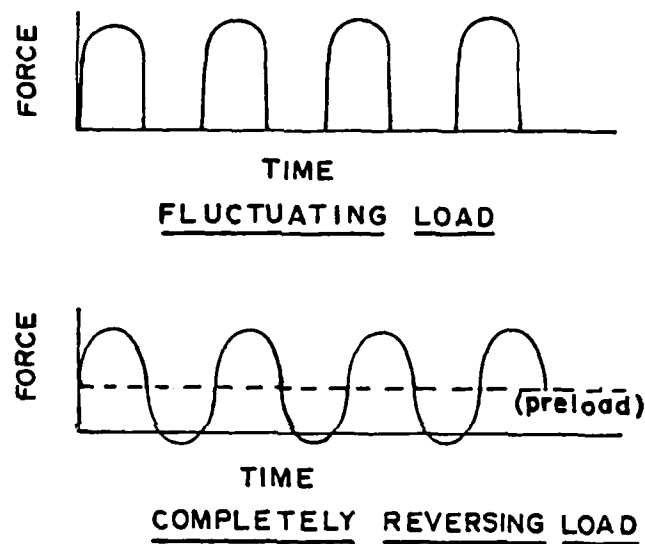
Figure 3.1 Comparison of Types of Fluctuating Load

Many theories exist that try to explain the phenomenon of fatigue failure, most of them in agreement that microscopic cracks form at places where high localized stresses occur. The cracks become progressively larger each time the load is applied until they grow together to form visible cracks in the material, and the part subsequently begins to fail. Since the tiny cracks form each time a certain level of stress is reached, the frequency of application of load

occurs under repeated loading is commonly referred to as fatigue failure.

3.2 Factors Affecting Material Failure

3.2.1 Fatigue Failure

Material failure due to fatigue became of interest in the mid 19th century about the time the steam engine developed. Machinery of earlier periods involved relatively slow speeds and light loads, and the strength of materials used was generally judged entirely on the basis of static considerations. This method proved adequate until it was noticed that railroad axles which were designed based on static analyses were failing prematurely [7].

W.J.M. Rankine [8] discussed the railroad axle problem in a paper in 1843, which in effect was the genesis of serious discussion of fatigue. Rankine and his contemporaries were concerned with a type of repeated loading called completely reversing load, where the applied load changes from a peak in one direction to the same magnitude in the opposite direction. Completely reversing load can often be represented as a sine function with the magnitude of load or stress fluctuating about the value of preloading in the system.

CHAPTER 3 - STRENGTH OF MATERIAL ESTIMATES

3.1 Introduction

The strength of the locking shoulder/restraint combination is its ability to withstand a particular input load. Although the input load may not change, the strength of the part and rivets may change since moving or removing restraints will change the effective area of the material in shear or compression, and may alter locations and magnitudes of high stress concentration areas.

To estimate the strength of the fasteners and restraints it must be understood that the load they will sustain is dynamic/impact and if failure occurs it will most likely be due to the effects of repeated loading. Since failure due to repeated loading occurs at stresses well below the static elastic strength of the material, a static analysis of the system by itself is inadequate [7]. However, a prediction of the estimated life of the part can be made based on a knowledge of the stress produced by the maximum load on the part, an estimate of the stress impact factor, and the application of methods of analysis of repeated loading of structural elements. Failure that

Since there are two locking shoulders,

$$f_{applied_x} = \frac{3676 \text{ lbs}}{2} = 1838 \text{ lbs} \qquad (2.7)$$

and

$$f_{applied_y} = \frac{-1054 \text{ lbs}}{2} = -527 \text{ lbs} \qquad (2.8)$$

The effect of the applied forces on the strength of the locking shoulder will be dependent on the manner in which they are dynamically applied. The dynamic and impact factors of the loading are addressed in the next chapter.

BOLT
ASSEMBLY
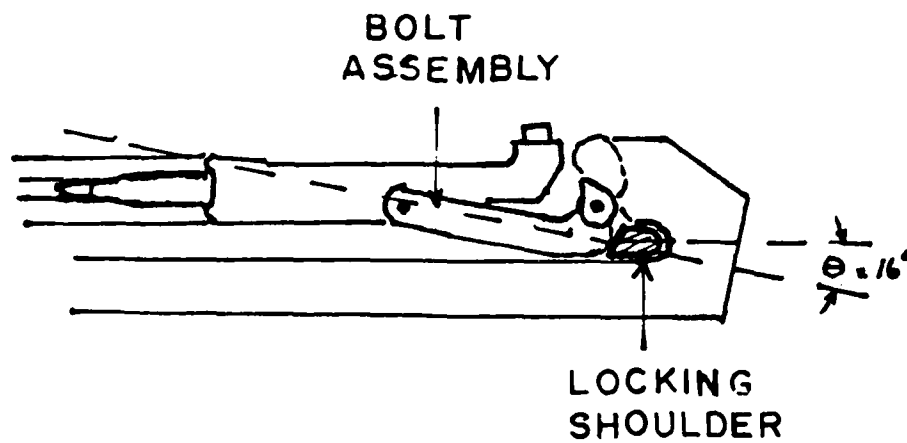
LOCKING
SHOULDER

Figure 2.11 Gun Mechanism in Locked Position
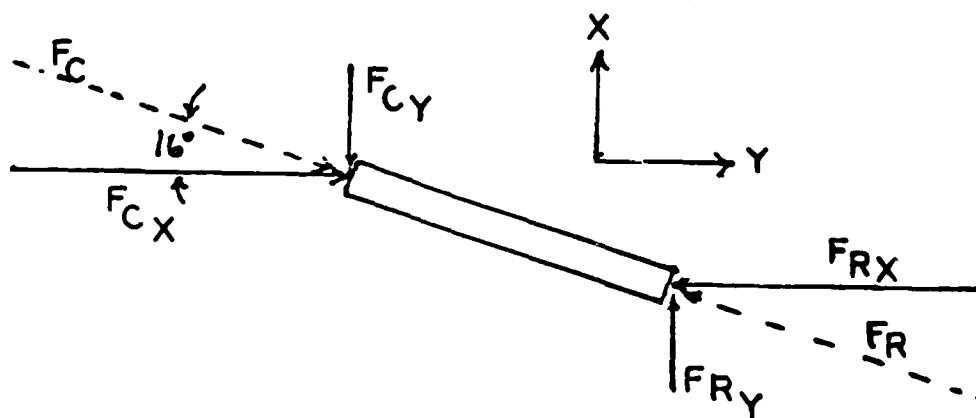
Figure 2.12 Free Body Diagram of Bolt Carrier

This force in the cartridge is transferred through several parts to the locking shoulder. The configuration of the contacting parts determines the vector component of the force of the cartridge ($f_{c_{max}}$) that acts on the locking shoulders.

The free body diagram in figure 2.12 is extracted from figure 2.11. From the free body diagram, $f_{c_x} = f_c \cos 16$ degrees, and $f_{c_y} = f_c \sin 16$ degrees. Since $f_{c_x} = f_{c_{max}} = 3676$ lbs, $f_{c_y} = -f_{c_{max}} \tan 16$ degrees $= -1054$ lbs.

The force analysis based on the free body diagram in figure 2.12 assumes $\Sigma F = 0$ for the bolt instead of $\Sigma F = m\ddot{x}$. This assumption is made since the acceleration of the bolt in this case is unknown and clearance between the bolt and chamber and between the bolt and locking shoulder vary slightly from one weapon to the next. The resulting force on the locking shoulder from the bolt under the assumption of static force application will be higher than the actual force which is dynamically applied, since the inertia of the bolt will resist the force application. Therefore, the static analysis provides a conservative estimate of the force transfered through the bolt to the locking shoulder.
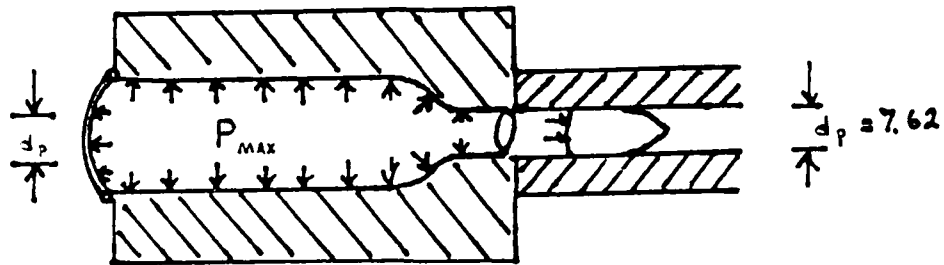
Figure 2.9   Pressure Schematic

$$\therefore$$

FORCE ON BOLT = ^-F_P

$$= F_{C_{MAX}}$$
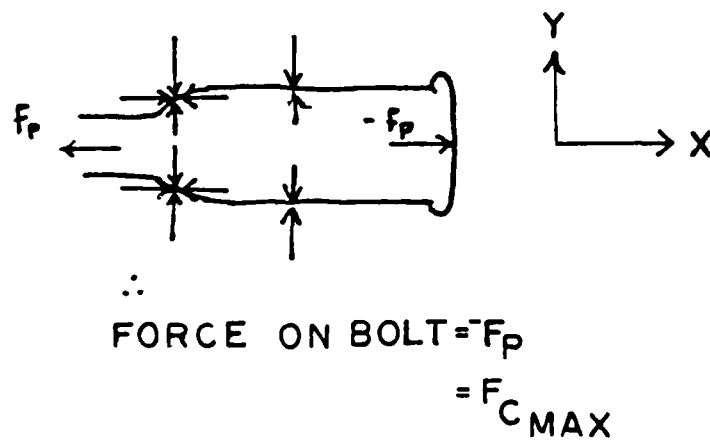
Figure 2.10 Free Body Diagram of Forces on Bolt
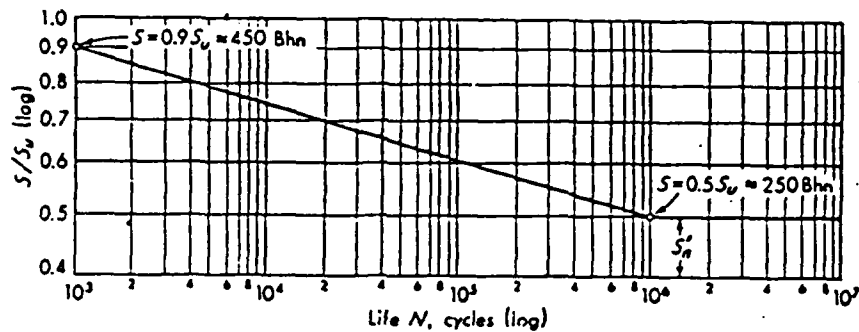
Figure 3.2 Generalized S-N Curve for Wrought Steel [8]

Applying the stress impact factor gives $K_i S = .5S_u$ or $S = .2 S_u$.

From the 1981 Materials Selector [12], S_u for AISI 1010 carbon hot rolled steel is 47,000 psi, and S_u for AISI 9310H steel is 168,000 psi. Substituting values gives $S_{rivet_{max}} = 9400 \frac{lbs}{in^2}$ and $S_{locking\ shoulder_{max}} = 33,600 \frac{lbs}{in^2}$

3.3 Calculation of Stress in Fasteners and Restraints

To find the stress in any of the fasteners or res-traints the fraction of the overall load carried must be determined. In this case, since the load from the locking shoulder passes through several parallel paths, the problem is statically indeterminate. Once the load on the indivi-dual rivet or restraint is known, the area over which it

acts must be found, and the stress calculated accordingly.

3.3.1 Distribution of Load Between Rivets

It is commonly assumed that the load in a row of rivets is divided equally among them when it is applied along the line formed by the row. This is a valid assumption when the two plates are much stiffer than the fasteners. Transverse loading of rivets is a statically indeterminate problem that is difficult to solve if this assumption is not made. This assumption is not truly valid, however, and most notably cannot be made if there is any eccentricity to the rivet group loading. A more precise understanding of load distribution is gained by observing the moments produced by the resistance of the rivets to an eccentrically applied load.

The method presented here is based on an approach to the analysis of riveted joints presented by F.R. Shanley [13]. As stated above, many simplifying assumptions must be accepted if a useful solution is to be obtained by this method. It is assumed in this case that friction between the riveted plates is zero, and clearance between each rivet and rivet hole is zero. The validity of these assumptions was discussed in section 3.2.

Consider figure 3.3. Resistance to deformation is nearly linearly proportional to minimum strength in shear

or bending if the loading remains beneath the proportional limit of stress. If we assume linear proportionality, then it follows that resistance to deformation is also proportional to the cross-sectional area of the rivet. Thus the total cross sectional area of the rivets in shear will be proportional to the total resistance force produced by the rivets. Therefore,

$$\Sigma M_c = \overline{F}_A d_o \tag{3.5}$$

where

M_c = moment about the centroid caused by the resistive forces of the rivets

$\overline{F}_A$ = applied force

d_o = distance between centroid and point of application of F_A

In the specific case under consideration here, due to symmetry around the horizontal line through the rivet holes, the y coordinate of the centroid is the same as the y coordinate of the center of the holes. The x coordinate is found from the relation

$$d_{o_x} = \frac{\Sigma A_i x_i}{\Sigma A_i} \quad i = 1,n \tag{3.6}$$

where
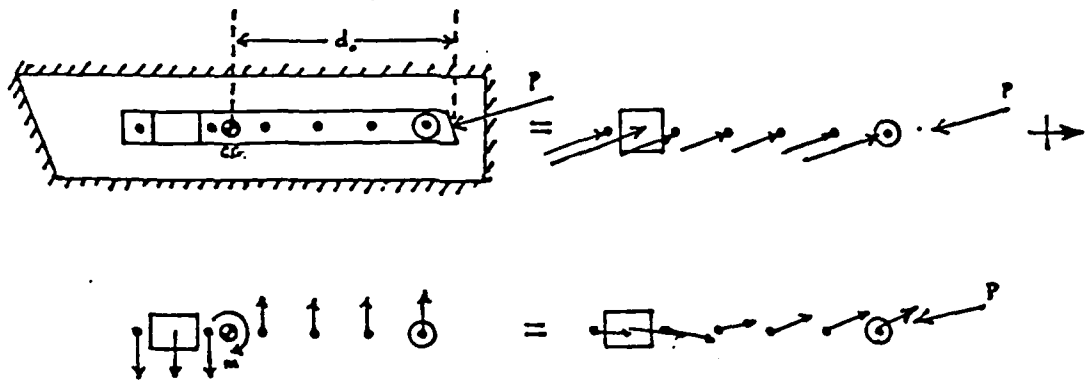
Figure 3.3 Eccentrically Loaded Rivet Group

d_{o_x} = location of centroid of areas of restraints in shear in the x direction from the origin of the local coordinate axes

x_1 = location of center of individual shear area along the x axis

A_1 = cross sectional area of the restraint in shear

n = number of restraints

Since d_{o_y} = 0, d_o = d_{o_x}.

The direct load resisted by each rivet will then be given by the vectors:

$$\overline{P}_{d_1} = \frac{A_1}{\Sigma A_1} \overline{P} \qquad (3.7)$$

$$\overline{P}_{d_2} = \frac{A_2}{\Sigma A_i} \overline{P} \qquad (3.8)$$

.

.

.

$$\overline{P}_{d_n} = \frac{A_n}{\Sigma A_i} \overline{P} \qquad (3.9)$$

$$i = 1, n$$

For rotation about the center of gravity the deformation of each rivet is proportional to its distance from the center of gravity. Hence the moment resisted by each rivet will be

$$M_i = \frac{A_i r_i^2}{\sum\limits_{j=1}^{n} A_j r_j^2} \overline{P} \, d_o \qquad (3.10)$$

where

i = rivet being studied

n = number of rivets

r = distance from rivet center to centroid

The loads due to moment will therefore be

$$\overline{P}_{m_i} = \frac{M_i}{r_i} = \frac{A_i r_i}{\sum\limits_{j=1}^{n} A_j r_j^2} \overline{P} \, d_o \qquad (3.11)$$

The total load on a rivet then is the vector sum of the load due to moment and the direct load.

$$\overline{P}_{i_{tot}} = \overline{P}_{d_i} \mathbin{+\mkern-8mu\rightarrow} \overline{P}_{m_i} \qquad (3.12)$$

The location of the centroid of the restraint shear areas will change if the T-slot at the rear end of the locking shoulder is widened, since the effective area in shear in the y direction will change. The locations of each centroid have been calculated and are shown in figure 3.4.

Direct loads resisted by rivets and restraints of the locking shoulder must be calculated by considering the separate application of the vector components of the input force $F_{applied}$. This is necessary since the restraint in the T-slot will carry load applied along the x-axis over its entire area in shear, while load applied along the y-axis will only be carried by part of the shear area of the restraint in the original design. In the modified design the restraint in the T-slot will carry no load in the y direction.

Loading due to moment must also be calculated by separating the input force into components for the same reasons as stated for direct loading. Since $d_{o_y} = 0$, total resistance due to moment will be found by using the y component of input force.

The magnitudes of the loads carried by each rivet and restraint due to direct loading and moment are listed in table 3.1. The amount of load on each rivet or restraint is shown as the fraction of total load, $F_{applied}$, that was determined in calculations for chapter 2 to be applied to the locking shoulder face. The direction of application of direct load is 16 degrees for all cases except the rear restraint in the new design, which is zero degrees. Moment loads are applied downward if the sign is negative and upward if the sign is positive. The words 'old design' and 'new design' in the table refer to the conditions prior to T-slot modification (old design) and after T-slot modification (new design).

Table 3.2 lists the magnitude of the total force felt by each rivet and restraint. No direction is indicated for table 3.2 since direction of force application is not important. The critical factors are the amount of load and the area over which it acts. The areas over which the forces are felt is discussed in the next section.
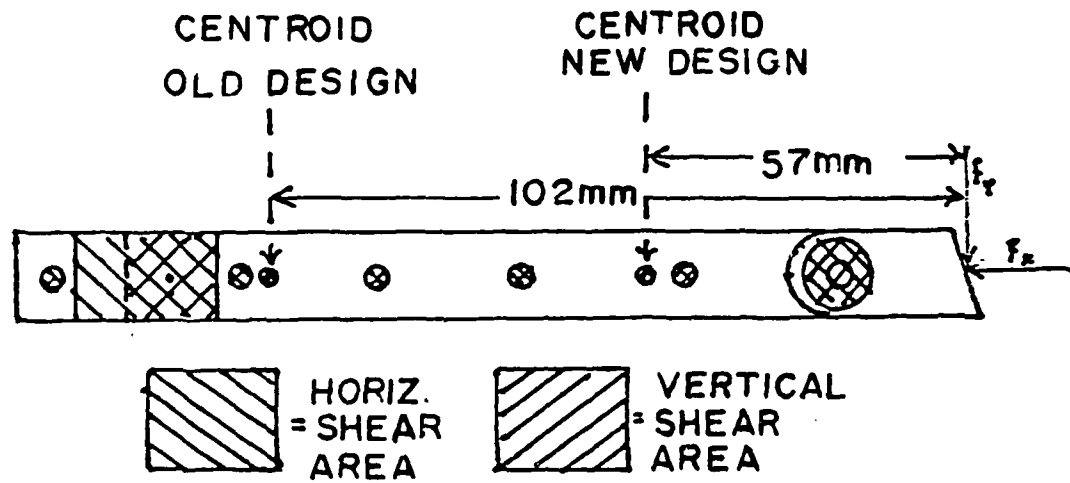
Figure 3.4 Location of Centroids of Areas in Shear

Table 3.1   Restraint Loads - Direct and Moment

Restraint Loads				
	Old Design		New Design	
Restraint	Direct	Moment	Direct	Moment
Forward	.169|F|	.0403|F|	.201|F|	.0476|F|
Rivet 6	.056|F|	.0132|F|	.066|F|	.0156|F|
Rivet 5	.034|F|	.0053|F|	.040|F|	.0025|F|
Rivet 4	.034|F|	.00256|F|	.040|F|	-.0045|F|
Rivet 3	.034|F|	-.0002|F|	.040|F|	-.0115|F|
Rivet 2	.034|F|	-.0030|F|	.040|F|	-.0185|F|
Rear	.715|F|	-.0478|F|	.613|F|	0
Rivet 1	.034|F|	-.0063|F|	.040|F|	-.027|F|

Table 3.2 Load Magnitudes on Restraints

Load Magnitudes		
Restraint	Old Design	New Design
Forward	.1840|F|	.2190|F|
Rivet 6	.0610|F|	.0719|F|
Rivet 5	.0358|F|	.0408|F|
Rivet 4	.0348|F|	.0390|F|
Rivet 3	.0339|F|	.0385|F|
Rivet 2	.0333|F|	.0392|F|
Rear	.7300|F|	.6130|F|
Rivet 1	.0328|F|	.0416|F|

3.3.2 Determination of Stress in Restraints

Consider figure 3.5. The stress across the diameter of a restraint in shear is called the cross shearing stress and is denoted by τ_{css}, where $\tau_{css} = \dfrac{F_s}{A_s}$. F_s is the applied load on the restraint, and A_s is the area of the restraint in shear.

The bearing stress σ_b is the normal stress in the rivet or restraint. For relatively thin plates, it is common to assume $\sigma_b = \dfrac{F_b}{A_b}$, where F_b is the load applied to the rivet and is the same as F_s, and A_b is the area bearing the load and is found by $A_b = td$ where $t =$ the thickness of the plate and $d =$ the diameter of the rivet hole [7]. Note that the area of concern is the projected area of the rivet, not the total area of contact.

Table 3.3 lists the restraints and rivets and their associated values of τ_{css} and σ_b. Values in table 3.3 were calculated using the force vectors listed in the previous tables.
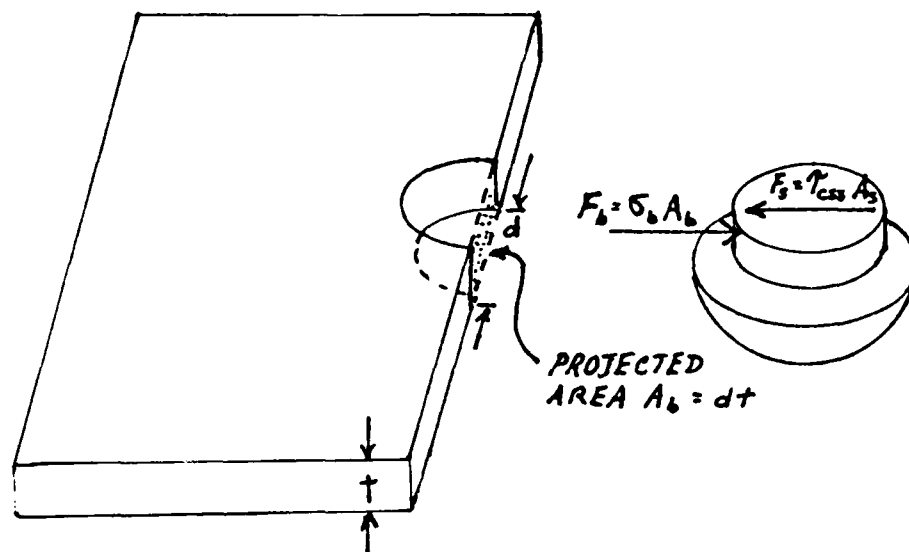
Figure 3.5 Cross Shearing and Bearing Stresses

Table 3.3 Rivet and Restraint Stresses

Stress Magnitudes (psi)				
	Old Design		New Design	
Restraint	σ_b	τ_{css}	σ_b	τ_{css}
Forward	-4839.2	2137.3	-5759.8	2543.9
Rivet 6	-3227.9	2159.9	-3804.7	2545.2
Rivet 5	-2426.3	2079.3	-2765.2	2369.7
Rivet 4	-2358.5	2021.2	-2643.2	2265.2
Rivet 3	-2297.5	1969.0	-2609.3	2236.1
Rivet 2	-2256.9	1934.1	-2656.7	2276.8
Rear	-19,199	2181.7	-16,122	1832.1
Rivet 1	-2223.0	1905.1	-2819.4	2416.2

3.3.3 Determination of Maximum Principle Stresses

Since the locking shoulder and the rivets are made from different materials, both the maximum principle stress in the rivets and the locking shoulder must be determined. The values must be compared to the maximum allowable stress in each material that were determined earlier. If failure occurs in any of the rivets or restraints, it will occur where the principle stresses are highest. Stress will be highest in the rivet or restraint that has the highest values for σ_b and τ_{css}. From table 3.2, that occurs in rivet 6 and the rear restraint in both the original design and the modified design.

From Mohr's circle,

$$\sigma_{max,min} = \frac{\sigma_x + \sigma_y}{2} \pm \sqrt{\left(\frac{\sigma_x - \sigma_y}{2}\right)^2 + \tau_{xy}^2} \qquad (3.13)$$

Table 3.4 lists the values of the principle stresses that were found by using equation 3.13.

From the von Mises-Hencky maximum distortion energy theory, for the structure to be safe,

$$\sigma_f > \sqrt{\sigma_1^2 - \sigma_1 \sigma_2 + \sigma_2^2} \qquad (3.14)$$

where σ_f is the stress that will cause failure, in this case, $.2\ S_u$. Also, σ_1 and σ_2 are the principle stresses. Setting $\sigma_1 = \sigma_{max}$ and $\sigma_2 = \sigma_{min}$ gives the following :

rivets are joined to both the locking shoulder and the receiver. Therefore the elements of the model are correctly connected.

DISTORTION ≈ 1.0   DISTORTION ≈ 0.5
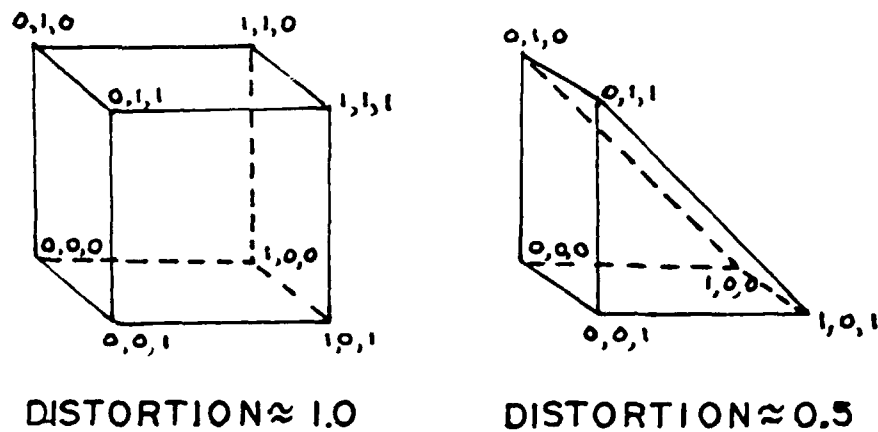
Figure 4.4 Element Distortion Check

4.3.2.3 Free Edge Check

Once all coincident nodes have been merged and element distortion is checked, a ´free edge´ drawing of the model should be drawn to insure there are no separations between model sections. When two nodes are connected in such a way that they do not share the same edge as any other element, they are considered a free edge.

A free edge drawing of the locking shoulder/rivets/receiver wall model in figure 4.5 shows that the outer edge of the locking shoulder is drawn along the surface of the receiver wall. This demonstrates that the locking shoulder and receiver are not joined. However, there are no free edges shown where rivets exist, since the

part sections, the nodes on the surface of one part section must coincide with the nodes on the surface of the part section with which it is to be joined.

In GRAFEM it is possible to change the global coordinates of nodes by picking or selecting nodes by label number, and assigning the new coordinates. Mesh that is drawn between nodes to be moved is erased by the computer and redrawn to the node in its new location.

Once the surface nodes of part sections are coincident, they must be merged so the mesh from one section will join with the mesh from the other section. In GRAFEM this is done simply by entering the CHECK menu and selecting the coincident node check option. The command to merge coincident nodes is given once the computer locates them.

4.3.2.2 Element Distortion

The shape of each element in the model must be checked for distortion. The mathematics of the finite element analysis requires that the correlation between optimal element shape and actual element shape be no less than .25 [17]. See figure 4.4. Optimal element shape is found by using isoparametric shape functions to determine the best shape for a particular element type. This check can be performed in GRAFEM by choosing the ´distortion´ option from the CHECK menu.

4.3.2 Model Construction

The finite element model of the locking shoulder was constructed by creating several GRAFEM planes, each representing one face of a section of the part. Boundary nodes were placed on the boundaries that defined each plane, as well as the boundaries that defined any holes in the plane. Mesh was generated between nodes and was extruded, or swept, through space along a vector that defined the width of the part section. The groups of elements defined by the separate planar extrusions were then joined at the surfaces in contact.

Creation of boundaries, planes, nodes, and mesh is a straightforward process that is described in detail in the GRAFEM User's Guide. Techniques for joining part sections that were created from separate planes are not described in great detail in the user's guide. The following paragraphs discuss the considerations that are essential to assure proper model construction.

4.3.2.1 Coincident Boundary Nodes

As described above, a part can be thought of as a collection of part sections. The part sections must be joined to create the complete model. Each part section consists of three dimensional elements that are internally joined at the nodes on the corners of the elements. Thus, to join
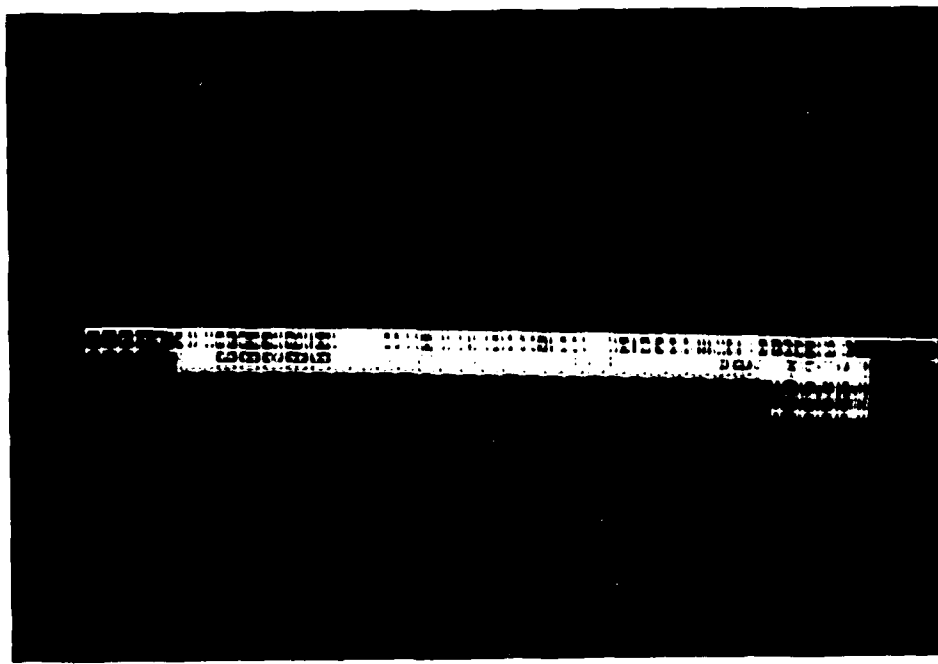
Figure 4.3 Finite Element Model - Top View

64

NOT AVAILABLE
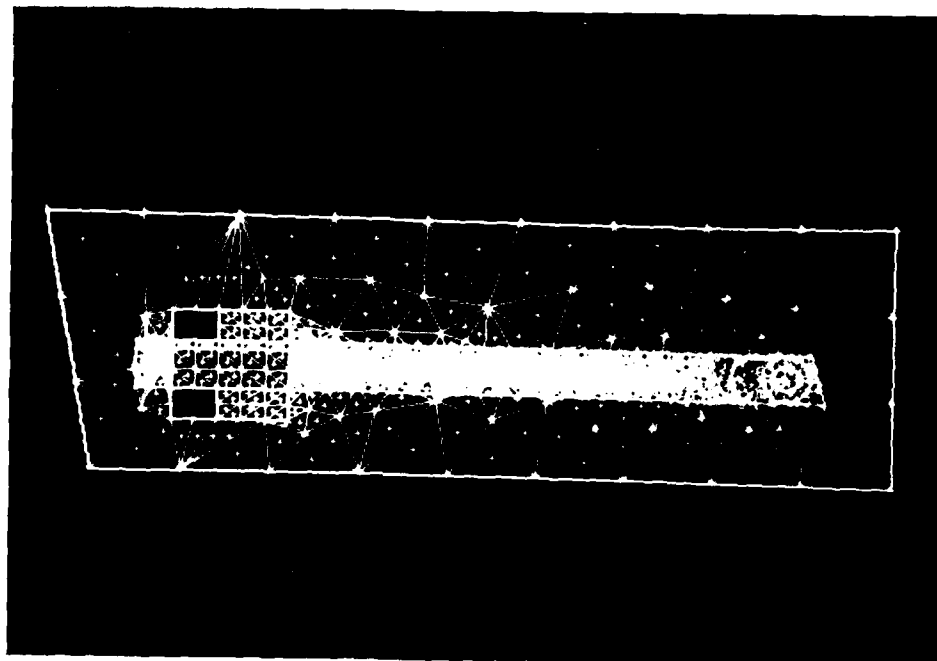
Figure 4.1 Finite Element Model - Isometric View

Figure 4.2 Finite Element Model - Front View

the hardware capability that is now available.

A recently developed finite element analysis package offered by Applicon includes a graphic finite element modeler (GRAFEM) and an interactive finite element analyzer (IFAD). GRAFEM/IFAD is an easy to use system that allows the user to create one, two, or three dimensional finite element models based on part geometry.[16] GRAFEM/IFAD is the system that was used to create and analyze a finite element model of the locking shoulder, fasteners, and receiver wall of the M240 machine gun.

4.3   Finite Element Model of Locking Shoulder

4.3.1   Description of the Model

Figures 4.1 through 4.3 depict the finite element model of the locking-shoulder/rivets/receiver combination that was created to represent the actual part. It is a three dimensional model consisting of 977 wedge shaped (6 noded) solid, linear, isoparametric elements. All nodes around the the outer perimeter of the large wall (representing the receiver wall) were restrained from motion in all 6 degrees of freedom. The amount of load applied to the face of the locking shoulder was determined by dividing the magnitude of the x and y components of applied force by 8, and applying the result to each of the 8 nodes on the face of the locking shoulder.

Some software packages in use today with personal computers are identical to or are descendants of systems that were developed for mainframe or minicomputers. The microcomputer normally does the same type of analysis that its larger relative does, with limitations placed on main memory space or disk storage. Often a problem can be broken into parts, the parts analyzed separately with results stored on disk, and the parts subsequently combined to obtain a final solution to a large problem. This method is sometimes inconvenient, however, and large jobs are still done on the more powerful machines.

Numerous analysis packages useful with minicomputers and mainframes are on the market. Two of the most widely used are ANSYS (Swanson Analysis Systems Inc.) and NASTRAN (National Aeronautics and Space Administration). Capabilities and descriptions of the most commonly used software packages have been compiled and are included in an excellent reference by C.A.Brebbia [16].

The popularity of a computer software package is often a function of its compatibility with existing hardware, its ability to solve a wide range of problems, and its age. As was implied in the discussion on use of microcomputers, hardware developments in recent years have provided computing power that exceeds early software developments, generating much activity by programmers in an attempt to use

until the recent advent of the relatively powerful but inexpensive minicomputer microcomputer. Until now the practicioner had to wait on programmers and data processing managers for answers to finite element analyses, making finite element modeling impractical for many problems. Relatively small material strength problems that did not require extreme precision were solved using techniques similar to those presented in chapter 3, and large factors of safety were applied to account for inaccuracies. With the increasing capacity of the minicomputer and microcomputer the tools for finite element analysis have been provided directly to the engineering workstation. The design engineer now needs only a limited understanding of the theory of finite element analysis and the ability to interpret results, to use the method for most common structural design problems.

Many finite element analysis packages have been and continue to be developed for personal computers. An excellent reference describing the most common software packages used with microcomputers, their capabilities and costs, is presented by Falk and Beard [15]. They compare several finite element analysis packages including FESDEC, GIFTS, LIBRA, CAEpipe/CAEframe, FiniteGP, Frame 2-D, Images 2-D/3-D, MSC/pal, SAP86, and SUPERSAP. Comparisons are based on types of analyses performed, interactive ability, preprocessing capability, graphics capability, and cost.

model of the structure and fasteners must be developed.

Results obtained from finite element analyses have often proven to be as accurate as those obtained from empirical testing. Care must be taken to insure the model is constructed to be an accurate representation of reality, however. This chapter presents an historical overview of the finite element method, and then describes the finite element model used in this study to predict the stresses in the locking shoulder and the rivets.

4.2   Finite Element Modeling - an Overview

The mathematics of the finite element method began development in the mid-nineteenth century with the concepts of framework analysis initiated by Maxwell, Castigliano, and Mohr [14]. Progress in the development of theory and analytical techniques that were prerequisite to the finite element method was slow until approximately 1920 when Maney and Ostenfeld developed truss and framework analysis based on displacement parameters as unknowns. Severe limits on the size of problems that could be handled by matrix methods existed until the digital computer was developed in the 1950's. Large matricies could then be manipulated with relative ease, and problems that were previously unsolvable in a practical sense could be solved.

Finite element analysis was the domain of the expert

CHAPTER 4 - FINITE ELEMENT MODEL

4.1 Introduction

Chapter 3 described an analysis of the strength of the locking shoulder and fasteners based on the assumption that the load is carried evenly across all areas in shear. This assumption is commonly made in the design of riveted joints since the statically indeterminate nature of the problem makes solution by any other method complex.

The assumption of uniform load distribution across areas in shear implies, among other things, infinite stiffness of the plates that are fastened together. However, it is intuitive that in this case the structure does deflect some. In fact it will be shown later that the load distribution among fasteners is non-uniform due to this deflection.

To account for the effects of finite stiffness of the structure and proximity of load application to the fastener, a complex spring-mass model must be developed to represent the structure and fasteners, and a set of simultaneous equations must be derived in the form of $\{F\}=\{K\}\{X\}$ for the masses in the model. In short, a finite element

3.4 Conclusions

From section 3.2, $S_{rivet_{max}} = 9400 \frac{lbs}{in^2}$ and $S_{locking\ shoulder_{max}} = 33,600 \frac{lbs}{in^2}$. The results from the preceding paragraph are well below these values for both the present design and the modified design. Although the amount of stress in rivet 6 increases with the design modification, a factor of safety of 1.61 still exists.

From the analysis described in this chapter, it can be concluded that the proposed modification in the T-slot may be made. However, some traditional assumptions were made that may not be entirely accurate. The validity of the assumption that the direct load is carried evenly by all fasteners based on area in shear is questionable since the bulk of an applied force, particularly an impact force that is applied and withdrawn extremely quickly, is felt by the restraint nearest the point of application of the load. The analysis described in the next chapter does not make this assumption and the results are significantly different.

Table   3.4 Principle Stresses

Principle Stresses (psi)		
Stress	Old Design	New Design
$\sigma_{max_{r6}}$	1082.3	1275.3
$\sigma_{min_{r6}}$	-3773.5	-5080.4
$\sigma_{max_{rr}}$	244.8	205.6
$\sigma_{min_{rr}}$	-19,443.8	-16,327.6

$$\sigma_{f_{r6_{old}}} > 4415.3 \ \frac{lbs}{in^2} \tag{3.15}$$

$$\sigma_{f_{r6_{new}}} > 5823.7 \ \frac{lbs}{in^2} \tag{3.16}$$

$$\sigma_{f_{rr_{old}}} > 19,567.3 \ \frac{lbs}{in^2} \tag{3.17}$$

$$\sigma_{f_{rr_{new}}} > 16,431.4 \ \frac{lbs}{in^2} \tag{3.18}$$

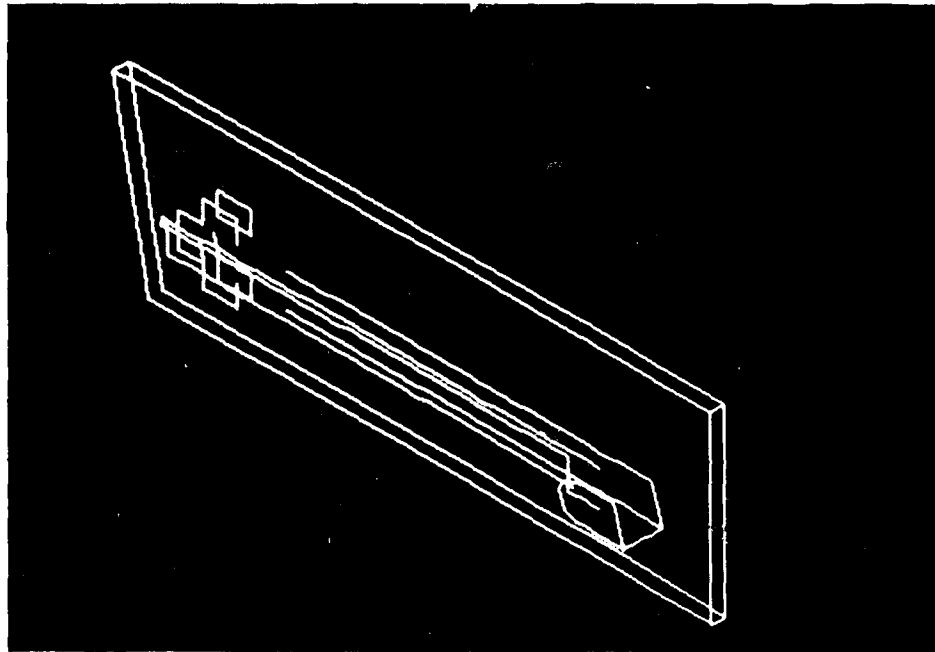where rr = rear restraint, and r6 = rivet #6.

Figure 4.5 Free Edge Drawing of FEM

4.3.3 Assumptions

Due to the complexity of the geometry and the fact that the structure actually consists of several separate parts it was necessary to make some simplifying assumptions prior to constructing the finite element model.

1. In an automatic weapon temperature increases drastically in the chamber area, barrel, and forward portion of the bolt. However, very little heat is transferred through the material of the receiver wall to the location of the locking shoulders. The weapon is normally employed by firing six to nine round bursts, with several seconds between bursts. This method prevents extremely high temperatures from forming, which is required in order to obtain a reasonable life of the barrel. Therefore it can be assumed that the receiver and locking shoulder temperature is constant and material properties are not affected.

2. All parts are made of steel. Although the steel used in the rivets has a different hardness and yield point than the steel used in the locking shoulder, the modulus of elasticity and shear modulus of all steels are very much the same at the same temperature. Values of $E = 29.5e6 \frac{lbs}{in^2}$ and $G = 11.4e6 \frac{lbs}{in^2}$ were assumed for the entire structure. Poisson's ratio was assumed to be .3, and weight density of steel $\gamma = .28 \frac{lb}{in^3}$ [8].

3. The receiver wall is actually larger and of a slightly different shape than the structure used to represent it in the finite element model, but the thickness of the wall in the finite element model is accurate and it is large enough to allow a close approximation of the stiffness contributed by it. The receiver wall is assumed to be effectively restrained around its perimeter since the receiver is considered to be the stationary reference frame for the purposes of this study.

4. The 8 separate parts of the locking shoulder/rivets/receiver wall combination were essentially combined into one part in the finite element model. An early attempt was made to create a model that allowed bending of the rivet and separation between the rivet and inner wall of the rivet hole. The complexity involved quickly defeated the purpose of creating a simple finite element model of the system. A complete discussion of the types of models considered and reasons for selecting the model presented herein as the final model are included in the following section.

4.3.4 Development of Final Model

The final form of the finite element model of the locking-shoulder/rivets/receiver group was chosen after consideration of several alternatives, which are described below. Included in the discussion are the relative

advantages and disadvantages of each model and the reason
it was not used.

4.3.4.1 Locking Shoulder Alone

The first attempt at determining the stresses in the
fasteners and restraints was to simply create a 3 dimen-
sional finite element model of the locking shoulder alone.
The stiffness of the rivets was to be represented by ground
spring elements connecting the nodes inside the rivet holes
with the ground. The advantages sought by use of this
method were reduced size of the model (thus reducing compu-
tation time), and accuracy of results.

Ground spring elements are nothing more than two-noded
linear beam elements that have been defined as springs
under GRAFEM. Stiffness in all 6 degrees of freedom for
each ground spring element must be known and assigned as an
element property in element property tables. The ground
spring element is most commonly used to represent the
stiffness of the mounts between a structure and a reference
frame or ground.

If the bending stiffness of the rivet inside the hole
could have been accurately determined this approach would
have given good results. The problem of determining rivet
stiffness under transverse loading, however, is complex. A
rivet loaded in shear can be modeled as a beam subjected to

a nearly parabolic load distribution on one side, with a reaction on the opposite side also being a parabolically distributed load. Rather than attempting an analytical solution to this difficult problem, it seemed logical to simply include the rivets in the model and allow the finite element modeler to predict the rivet behavior.

4.3.4.2 Locking Shoulder and Rivets Combined

Due to the complexity of the rivet stiffness problem, the next model considered was a finite element model of a combination of the locking shoulder and the six rivets. In this model the rivets were considered as integral parts of the shoulder similar to the forward and rear restraints. Restraints were placed on the 'posts' formed by the rivets, as well as the forward and rear restraints, and resulting stress at those nodes on the surface between the rivet and rivet hole were studied.

It was intended that wherever tensile stress occurred at these particular nodes, the elements would be separated at those locations and allowed to move freely, since only compressive forces exist between the locking shoulder and rivets. There are two reasons this was not done.

First, in GRAFEM, once nodes are merged they cannot be easily separated. Additionally, once restraints and forces are applied to a model and it is analyzed with IFAD, the

data base for the geometry of the finite element model is sealed. This was not a major problem, however, since it is possible to save copies of the files containing the finite element geometry of the parts prior to merging nodes and adding loads and restraints. However, merging individual nodes is a time consuming process that has to be accomplished manually. The tedium of the task was obviously undesirable, although it would have been done if it were considered necessary.

The second and most important reason this task was not completed was that results from the initial analysis with all coincident nodes merged indicated that, in this particular case, it was not necessary. The forward restraint of the locking shoulder proved stiff enough to absorb almost all of the load by itself. Virtually no stress was felt further back than the first rivet behind the locking shoulder face, and that rivet experienced very little. Under the circumstances, the model in its present form gave results very close to those expected from a model with surface nodes of the rivets separated from the shoulder when in tension.

4.3.4.3 Locking Shoulder/Receiver/Rivets Combined

The model of the locking shoulder/rivet combination assumed infinite stiffness of the receiver wall. An improvement of this model was made by adding elements to

represent the wall, thus creating the final model used in this analysis, which was shown in figures 4.1 through 4.3.

In this model the stiffness of the receiver wall was adequately represented by the added elements. Values for stress that were obtained by use of this model were more accurate than those from the other models considered. Thus it was decided to use this model for the final analysis presented in this thesis.

4.3.5 Discussion of Results of Finite Element Analysis

4.3.5.1 Summary of Results

Figures 4.6 through 4.8 depict the stress contour lines as determined by a *von Mises-Hencky* maximum distortion energy stress analysis of both the original design and the modified design. The results of both the original and modified design are identical, thus the pictures shown represent both cases. The maximum distortion energy stress from the model is σ_{max} = 17,219 psi. The red contour lines in figures 4.6 through 4.8 depict values of stress between 13,180 psi and 15,820 psi. Yellow represents stress between 10,550 psi and 13,180 psi, green represents 7910 psi to 10,550 psi, light blue represents 5270 psi to 7910 psi, and blue represents 2640 psi to 5270 psi. Where there are no contours drawn, the value of stress is less than 2640 psi. The highest stresses occur at the forward portion of the

locking shoulder with very little of the magnitude of the stresses transmitted to the rear portion of the shoulder.

Figure 4.9 shows clearly that the largest distortion energy stresses are at the lower region of the front of the locking shoulder. As force from the bolt is applied to the locking shoulder face, the shoulder tends to bend inward toward the opposite shoulder it is matched against. This causes a large amount of compressive stress at the area indicated in red in the figure.
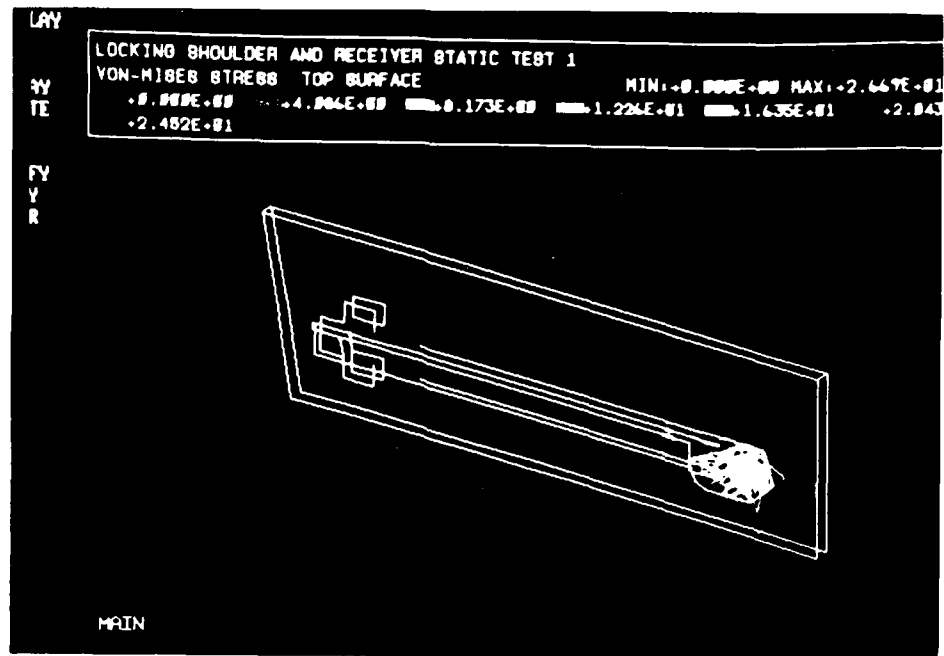
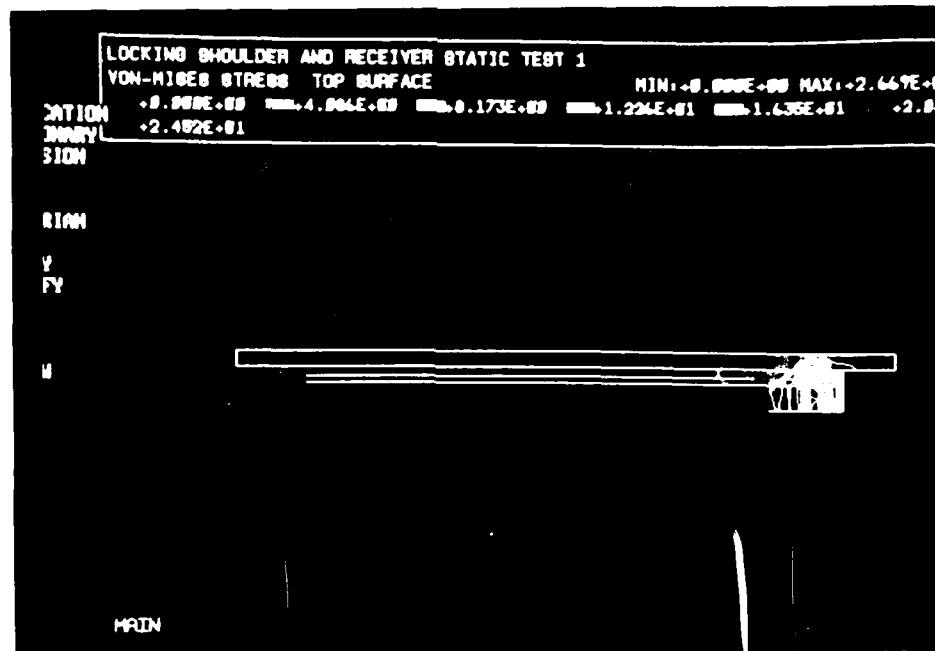Figure 4.6 von Mises-Hencky Stresses - Isometric
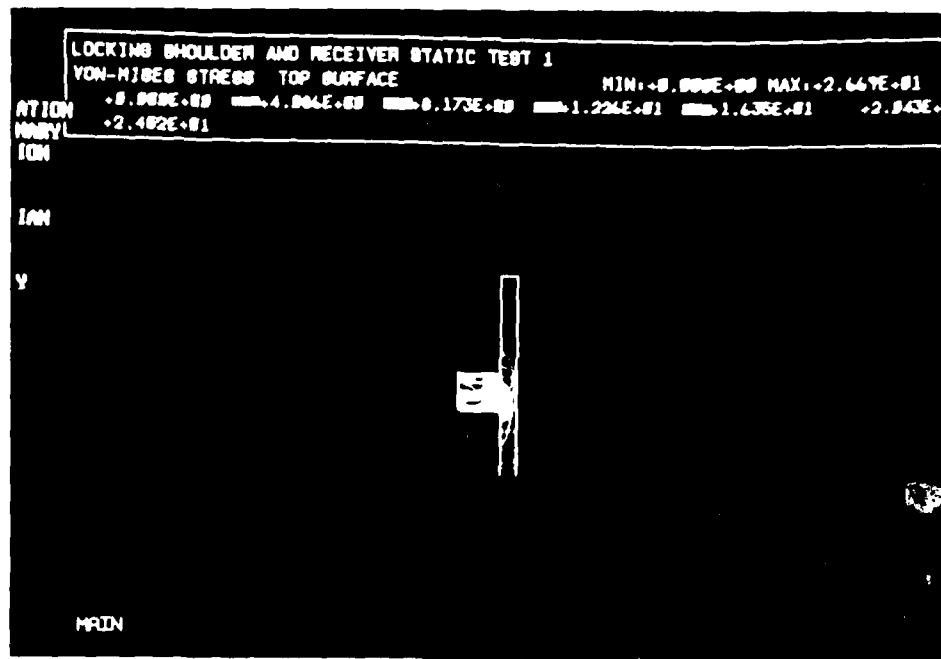

Figure 4.7 von Mises Hencky Stresses - Top

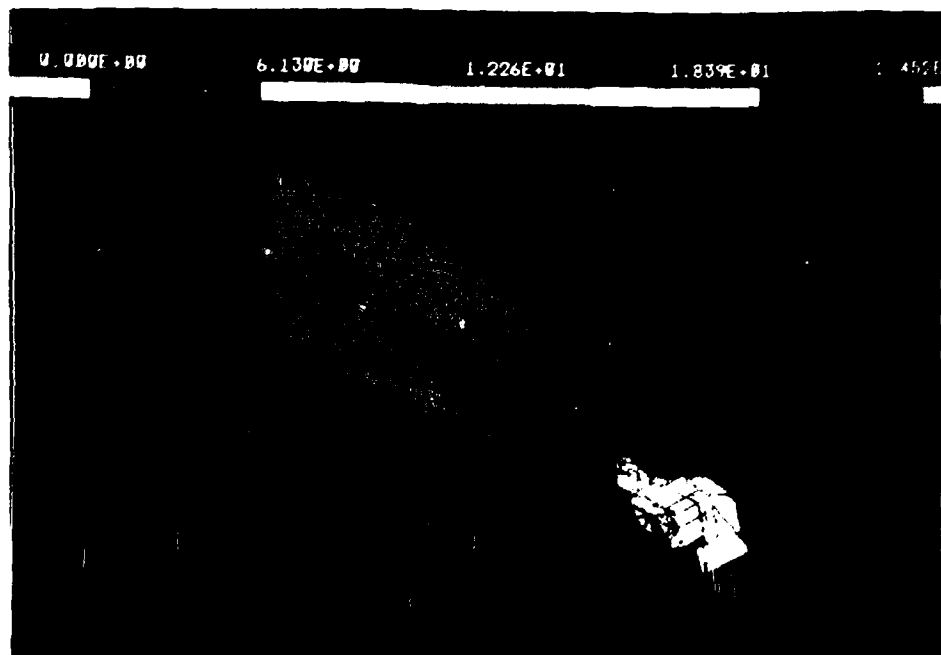Figure 4.8 von Mises Hencky Stresses - Side

Figure 4.9 Shaded Stress Contours

4.3.5.2 Conclusions

Conclusions to be drawn from these results include the following.

1. The desired modification of the T-slot can be made with virtually no adverse effect on the performance of the weapon. No values of stress in any of the elements changed measurably due to the modification. In fact, as was already pointed out, no stress due to loading is felt in the part of the locking shoulder near the rear restraint.

2. Based on the maximum allowable value of stress in the locking shoulder that was estimated in chapter 3, the life of the locking shoulder/rivet combination is very high. Maximum allowable stress for 10^7 cycles was estimated to be $33,600\frac{lbs}{in^2}$. Understanding that $\sigma_{max} = 33,600\frac{lbs}{in^2}$ is an estimate, it provides for a factor of safety of 1.95, a fairly high factor that would support the claim that the life of the locking shoulder will not be a limiting factor of the life of the weapon.

It is clear that there is a large difference between the results obtained with the finite element analysis and the results obtained in chapter 3. A comparison of the two methods and a discussion of the relative merits of each is the topic of the next chapter.

CHAPTER 5 - CONCLUSIONS AND RECOMMENDATIONS

5.1   Discussion of Models

Two models representing the locking shoulder, fasteners, and receiver have been presented. Chapter 3 described an approach often taken in the study of rivet groups, which assumed each fastener or restraint carries a fraction of the load proportional to its shear area. The finite element analysis described by chapter 4, however, did not make this assumption and the results were significantly different.

The disparity between the two models is large. The difference between them is a function of the validity of the assumptions made in the modeling process, and the analysis techniques used in each case. This chapter includes a discussion of those assumptions and analyses.

5.1.1   Load Distribution Between Rivets

The actual load distribution among a row of rivets obviously is not even. Figure 5.1 depicts the nature of the true load distribution [7]. It can be seen that the rivets on the ends of the rivet row carry considerably more of the

load than the rivets furthest from the source of the load. It has been recognized for some time that this is the case, and there have been many attempts to develop a practical method for calculating the exact load in each rivet [7]. As was indicated in chapter 3, however, the statically indeterminate nature of this problem makes a closed form solution very difficult.

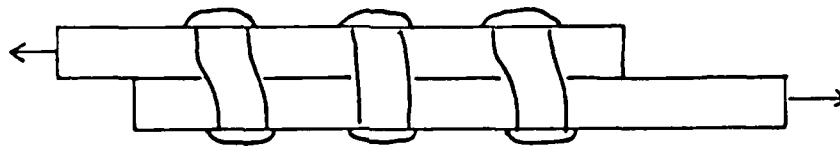Figure 5.1   Rivet Bending Under Transverse Load

It is possible to more evenly distribute the magnitude of stresses in the rivets by redesigning the fit of the joint. Consider the design shown in figure 5.2. In this joint the magnitude of stress across the entire joint is more evenly distributed between the rivets than it was in the more conventional joint shown in figure 5.1. The reasons for this include:

1. In this joint the bearing area of each rivet with the plate is increased where the transverse load is greatest. Remembering the analysis of chapter 3, it is clear that the normal stress $\sigma = \dfrac{F_{rivet}}{bearing\ area}$ is more nearly constant. Since principle stresses in the joint are proportional to the normal stresses, principle stresses will also be more nearly constant throughout the rivets.

2. Since the plate is thinner near the ends of the joint, it is stretched further, which allows the rivets near the center of the joint to take more load. Thus, all rivets tend to take equal load, and have equal stress, making the joint more efficient.
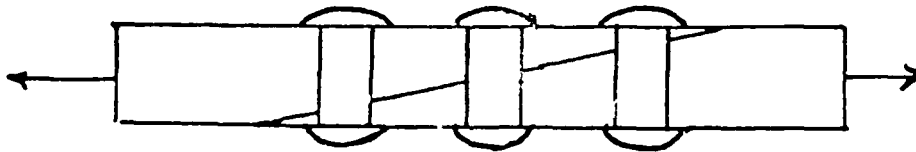
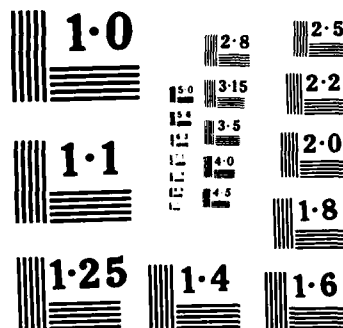Figure 5.2   Modified Riveted Joint

1·0

2·8

2·5

3·15

2·2

3·5

2·0

4·0

1·8

1·1

1·25 1·4 1·6

NATIONAL BUREAU OF STANDARDS
MICROCOPY RESOLUTION TEST CHART

Although a joint designed similarly to the one shown in figure 5.2 affords a more efficient use of available shear area of the fasteners, the strength of the plates between rivets is reduced where the plate becomes very thin. However, since the loads are less at these locations, the reduced strength of the wall is not a significant problem. The effort involved with shaping the fit of the plates often causes this type of design to be impractical, which is a major reason this type of joint is generally not used.

5.1.2 Load Application and Restraints

In the previous discussion, both plates of the joint were evenly loaded, in which case it is often acceptable and necessary to assume evenly distributed load across all areas in shear, as long as true behavior of the joint is understood and factors of safety are applied accordingly. This type of joint is probably the one most commonly encountered. It is found in most structures such as bridges, towers, pressure tanks, and light weight structures such as aircraft bodies.

The riveted joint of the locking shoulder and receiver of the M240 machine gun is a special case. Since one of the plates is so much larger than the other, and is mounted to a massive structure by very large pins, this large plate is for all practical purposes restrained to the ground, and infinitely rigid compared to the locking shoulder.

The relative infinite stiffness of the receiver wall prevents it from deflecting with the restraints and rivets of the locking shoulder. In a statically indeterminate problem, the magnitude of load felt at a location is normally proportional to the amount of deflection of the structure that is allowed at that location. It can be reasoned, therefore, that since the receiver wall is very stiff, the rivets and restraints that are behind the forward restraint will not be allowed to deflect very much, if at all. Since deflection in the rear restraints will be minimal, the load supported by these restraints will be very small. The results of the finite element model discussed in chapter 4 clearly support this reasoning.

5.1.3 Comparison of Results of Models

The total magnitude of distortion energy stress shown in the analysis of the preliminary model appears to be different than that given by the finite element analysis. There are two primary reasons for this.

1. The preliminary analysis was done using a hand calculator. Since it was intended only to be an estimate, all values were rounded off to no more than three significant digits. Calculations using the finite element model carried 13 significant digits in each calculation. Roundoff error in the preliminary model is significant.

2. Distortion energy stress in the preliminary model was calculated for a two dimensional case using two principle stresses and the shear stress that exists in the plane between the plates. The finite element analysis assumed three dimensions and calculated the distortion energy stress for each element from three principle stresses. Since the analyses in each case are different a comparison of the total magnitudes of stress from each analysis should not be made.

Clearly, the results of the finite element analysis are more accurate than the results of the preliminary model since fewer simplifying assumptions were made.

5.2 Conclusions

The results of the finite element analysis indicate that in the case of two fastened plates, one stiff and restrained and one less stiff and loaded, to assure adequate structural strength, the shear area of the fastener near the point of application of force should be large enough to withstand the total load by itself. This will provide more strength than necessary in the first restraint, but can usually be done if the need to minimize mass or size of the structure is not prohibitive.

In the specific case considered in this research, the rivets and restraint toward the rear of the locking

shoulder apparently contribute nothing to the structural strength, other than an additional safety factor and the application of normal force between plates to increase friction.

5.3 Recommendations

5.3.1 Design Modification Recommendation

Based on the results obtained by use of the finite element model and the conclusions discussed above, it is recommended that the proposed modification of the T-slot in the receiver be made.

5.3.2 General Recommendations

5.3.2.1 Finite Element Modeling of Rivets

The perspective of this study has been from the viewpoint of how to improve the design of a weapon that has already proven its reliability in the field. It was not necessary in this special case to improve the finite element model by accounting for the bending of the rivets. If finite element modeling is to be used to study riveted joints, it should be assumed in the general case that separation between the rivet and rivet hole must be accounted for.

5.3.2.2   Recommendations for Future Study

Future study in the area of riveted joints may benefit from the development of an empirical relationship between fasteners and load distribution. It may be feasible to develop a relationship with variables representing material properties, rivet diameters, plate thickness, and distance between rivets, based on either experimental results or results of finite element models.

5.4   Summary

A simple model of the interior ballistic activity of the M240 machine gun was developed to determine the forcing function applied to the face of the locking shoulder. Two models of the locking shoulder were developed, one a traditional approach assuming even distribution of load across areas in shear, the other a finite element model of the receiver wall, locking shoulder, and rivets. Both models were used to estimate the maximum stress in the part both prior to and after modification. The results of the models were found to be quite different, because of the lack of stiffness in the locking shoulder compared to the receiver wall. Both models indicate that the T-slot modification can be made without reducing the life of the weapon.

LIST OF REFERENCES

[1]   Chinn, George M. The Machine Gun Bureau of Ordnance, Department of the Navy, U.S.Government Printing Office, 1955.

[2]   Ehle, P.E. Mathematical Model of the Stoner 5.56 mm Medium Machine Gun, XM207" Technical Report 70-114, Science and Technology Laboratory, Research and Engineering Directorate, U.S. Army Weapons Command, October 1969.

[3]   Soifer,M.T. and R.S. Becker Dynamic Analysis of the 75 mm ADMAG Gun System S and D Dynamics, Inc.,Huntington, NY, December 1982.

[4]   Ehle, P.E., R.C. Huang, and E.J. Haug, Dynamic Analysis and Design of Weapon Mechanisms with Intermittant Motion" Procedings, Second U.S. Army Symposium on Gun Dynamics, U.S. Army Research and Development Command, Watervleit Arsenal, Watervleit, NY, September 1978.

[5]   U.S. Army Technical Manual TM 9-1005-313-34, Machine Gun, 7.62 mm, M240 April 1978.

[6]   FN Manufacturing Co., Inc. FNMI Test M240-C March 1983.

[7]   Higdon, Archie, E.H. Ohlsen, W.B. Stiles, J.A. Weese, Mechanics of Materials 2nd ed. John Wiley and Sons, Inc., New York, 1967

[8]   Juvinall, Robert C. Stress, Strain, and Strength McGraw Hill, New York, 1967

[9]   Department of Engineering, U.S.M.A. Weapon Systems Engineering - Elements of Armament Engineering U.S. Military Academy, West Point, NY, 1975

[10]   Spotts, M.F. Design of Machine Elements 5th ed.
        Prentice Hall, Inc., Englewood Cliffs, NJ, 1978

[11]   Timoshenko, S., and J.N. Goodier Theory of Elasticity
        2nd ed. McGraw Hill, NY, 1951

[12]   1978 Materials Selector Materials Engineering, Vol.
        86, No. 6, Mid-November 1977

[13]   Shanley, F.R. Basic Structures J. Wiley Inc., NY,
        1947

[14]   Gallagher, Richard H. Finite Element Analysis Funda-
        mentals Prentice Hall, Inc., Englewood Cliffs, NJ,
        1975

[15]   Falk, Howard and Charles W. Beardsley Finite Element
        Analysis Packages for Personal Computers Mechanical
        Engineering, Vol. 1, No. 1, January 1985

[16]   Brebbia, C.A., ed. Finite Element Systems Computer
        Mechanics Centre, Southampton, U.K. 1982

[17]   GRAFEM User's Guide Schlumberger Technology Corpora-
        tion, Burlington, MA, 1983

END

FILMED

7-85

DTIC